Effect of Monomer Structure and Compressibility on the Properties of Multicomponent Polymer Blends and Solutions: 1. Lattice Cluster Theory of Compressible Systems

Jacek Dudowicz and Karl F. Freed*

The James Franck Institute and the Department of Chemistry, University of Chicago, Chicago, Illinois 60637

Received December 4, 1990; Revised Manuscript Received February 19, 1991

ABSTRACT: The lattice cluster theory is extended to describe multicomponent mixtures of polymers with monomers that have internal structures and therefore extend over several lattice sites. One or more species of solvent molecules may be present, and the solvent molecules may likewise have internal structures. The excess (liquidlike) free volume in compressible systems is modeled through the presence of voids, unoccupied lattice sites that are smaller than the extended monomer structures. The algebraic complexity of treating the corrections to Flory–Huggins theory for the athermal limit packing entropy and particularly for the internal energy is considerably diminished by new developments, presented here. The algebraic representation of the lattice cluster theory enables proof of an important cancellation theorem for energy diagrams. We describe the methods for calculating the energy diagrams for multicomponent compressible systems, a special case of which is the two-component incompressible system for which results have been given previously without the derivation that is provided here for the more general case. The free energy is obtained from the lattice cluster theory as the sum of that for the compressible multicomponent FH theory and the noncombinatorial entropy and correlated energy corrections. The latter two contributions are obtained as a high-temperature expansion in powers of the ratios of the three independent van der Waals energies ϵ_{ij} to the absolute temperature k_BT. The coefficients in the expansion are further expanded in powers of z^{-1}, where z is the lattice coordination number. Contributions are evaluated through ϵ^2 and are obtained as simple power series in the volume fractions. Coefficients in this expansion are also dependent on monomer structure. Leading corrections are shown to violate the pairwise additivity assumptions of several standard phenomenological models of multicomponent systems. These corrections arise from local packing or interaction-induced correlations between segments of three or more species. The following paper applies the general theory to study the small-angle neutron scattering and excess thermodynamic properties of compressible structured monomer binary blends.

I. Introduction

Perhaps the most widely used theory for the thermodynamic properties of polymer melts, blends, concentrated solutions, etc. is the Flory–Huggins (FH) theory,[1] which has originally been formulated in terms of a lattice model. FH theory represents a simple mean field approximation to this standard lattice model in which all correlations are ignored in estimating both excluded volume effects and interaction energies. While classic FH theory successfully explains the fact that long-chain polymers in the liquid state generally tend to be immiscible, it is inadequate in several respects. First of all, it fails to describe the molecular origins of the substantial, temperature-independent (called entropic) portion of the small-angle neutron scattering Flory effective interaction energy parameter χ_{eff}, and it does not provide a molecular basis for the observed[2,3] composition dependence of χ_{eff} and other thermodynamic properties. Some of these inadequacies of FH theory may be traced to inherent limitations of the simple mean field approximation[1] embodied in FH theory.

In order to understand the origins of these deficiencies and to eliminate those that are not inherent in the lattice model, Freed and co-workers[4-8] have developed perturbative methods for systematically calculating corrections to the FH mean field approximation. The theory emerges in the form of a cluster expansion that bears a strong resemblance to Mayer's cluster expansion[9] for nonideal gases. Corrections to FH theory arise from packing- and interaction-induced local correlations between polymers, solvent molecules, etc. The noncombinatorial portion of the Helmholtz free energy for the lattice polymer system is generated *analytically* by the lattice cluster theory (LCT) as a single function of compositions, molecular weights, nearest-neighbor attractive van der Waals interactions, and temperature. The theory also includes a dependence on the individual monomer architectures, which are permitted to extend over several lattice sites and therefore more closely resemble actual monomer molecular structures.

Our recent comparison[10] of the LCT with Monte Carlo simulations of the lattice model for athermal limit packing entropies, internal energies of mixing, and coexistence curves for solutions of linear polymers in a single-bead solvent shows that the LCT provides the most accurate available thermodynamic description of these systems. Additional LCT computations[10] demonstrate that the internal energies of mixing and coexistence curves strongly depend on monomer and solvent molecular structures, reflecting alterations of nearest neighbor contact probabilities due to the local bonding. The general LCT formulas in our recent paper[10] apply also to incompressible binary polymer blends, but the current lack of computer simulations for these systems does not yet permit us to make a similar test of the LCT for incompressible blends, especially ones with structured monomers. The excellent accuracy of the LCT calculations for the polymer–solvent system, however, motivates the extension and use of this theory to describe polymer blends.

One limitation of the prior LCT calculations[10] for blends lies in the assumption of incompressibility. Polymer blends are liquids and therefore must be roughly as compressible as the corresponding monomeric fluids.[11] The importance of including compressibility has long been understood by those studying the thermodynamics of polymer systems. For example, compressibility implies that the nonathermal limit excess thermodynamic quan-

0024-9297/91/2224-5076$02.50/0

tities no longer depend on a single parameter ϵ, but depend separately[12] on all three individual interaction energies $\epsilon_{\mu\lambda}$ for a binary blend. This additional dependence arises because the creation of free volume in an incompressible blend destroys polymer–polymer contacts and thereby leads to a decreased energy.

The above deficiency of the recent LCT calculations[10] is removed here by generalizing the LCT theory to compressible multicomponent polymer mixtures, where solvent may correspond to one or more components. This generalization to multicomponent systems enables the treatment of arbitrary polydispersity distributions, but more importantly, it permits us to study how monomer and solvent molecule structures affect the thermodynamic properties of multicomponent systems, which become increasingly more tedious to study experimentally as the number of components increases. Many thermodynamic models[13] postulate that an appropriate interaction portion of the free energy of multicomponent systems may be represented as a linear superposition taken from the properties of the pure substances and binary mixtures. Our extension of the LCT to a multicomponent system therefore enables us to test such assumptions and to provide input information for modeling any nonadditive contributions if present.

The standard lattice model of a compressible polymer blend assumes that a lattice site may either be occupied by a monomer (i.e., a unit segment of a polymer chain) or remain vacant. Multiple occupancy of any lattice site is strictly forbidden. Our generalization of the lattice model allows a single monomer to occupy several neighboring lattice sites. Vacant sites are called voids and model the excess free volume[14] that must be present in any compressible system. Polymer chains of species $\mu = 1, 2, ..., k$ are represented by sequences of $\{N_\mu - 1\}$ main-chain bonds joining consecutive segments of species μ along with $M_\mu - N_\mu$ sites occupied by the units representing side groups. Lattice sites have z nearest neighbors, and all nearest-neighbor pairs of species μ and λ interact with van der Waals attractive energies $\epsilon_{\mu\lambda}$. The generalized lattice cluster theory provides the Helmholtz free energy for a compressible multicomponent system of polymers with structured monomers in the form of a double expansion in the inverse lattice coordination number $1/z$ and the reduced nearest-neighbor attractive interaction energies $\epsilon_{\mu\lambda}/k_BT$.

The original derivation[4,5] of the cluster theory uses field theoretic methods which are generally unfamiliar to polymer scientists. Our recent paper,[10] however, contains part of a new derivation for an incompressible binary polymer system that employs quite elementary mathematical methods. An additional advantage of this new algebraic derivation is that it enables us to make significant computational simplifications in evaluating thermodynamic properties of nonathermal mixtures. Here the algebraic representation of the LCT is further developed and is used to prove new theorems that further greatly reduce the computational labor involved in evaluating the internal energies. The focus of these developments is to simplify the generalization of the lattice cluster theory so that it may be applied to a multicomponent compressible system. These simplifications permit us to describe the evaluation of the higher order $\epsilon^n_{\mu\lambda}$ contributions to the internal energy that have been presented for incompressible systems in ref 10 without derivation.

The treatment of arbitrary chain architectures requires specifying monomer structures. Examples of these structures are given in Figure 1, where short chains are depicted

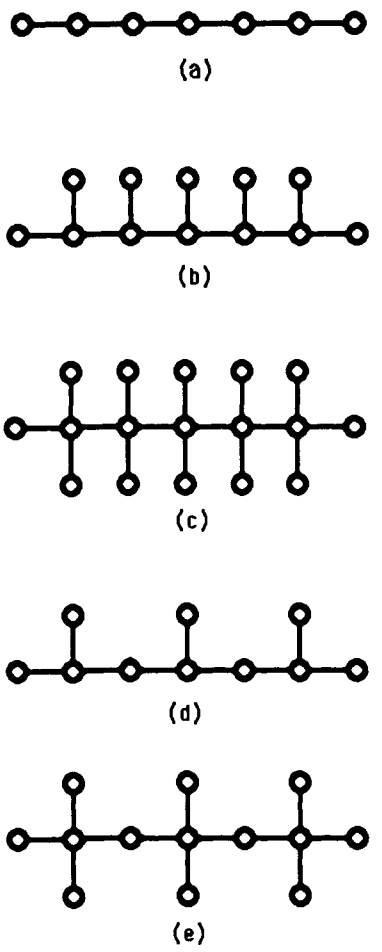

Figure 1. Sections of polymer chains with the same number $N = 6$ of backbone bonds, but with different monomer structures. Chains are drawn in two dimensions for simplicity, but all junctions are completely flexible in three dimensions. The architecture *a* represents a linear chain, whereas structures *b–e* are branched ones with monomers extending over a few lattice sites.

for simplicity and where the chains are assumed to be completely flexible at all junctions. Chains of a given architecture (i.e., of a given species) are all considered to have the same bonding topology and not to have closed loops. Treating such irregular, structured chains (or lightly cross-linked networks[15]) requires only the specification of certain counting indexes, described below in section IV. One or more of the components may be small solvent molecules whose structure is likewise specified through the same set of counting indexes.

Sections II and III, respectively, extend the algebraic derivation of the LCT for the athermal limit packing entropy and for the Helmholtz free energy of multicomponent compressible linear polymer mixtures, while section IV describes the generalization of the multicomponent algebraic LCT to models of polymers in which monomers have internal structures and are thereby allowed to occupy several lattice sites. The calculations are actually performed directly and quite generally for incompressible or compressible blends of different polymers with arbitrary architectures. The specialization in sections II and III to linear chains is provided solely to simplify the notation as much as possible in order to exhibit the salient content of the LCT and the mathematical methods employed. Analytical expressions are tabulated for the Helmholtz free energy of structured monomer, multicomponent, compressible mixtures. These analytical expressions enable the interested reader to consider applications to

ternary systems, polydispersity effects, phase diagrams, etc., fascinating applications that are too numerous for a few papers.

Typical behaviors for the LCT predictions of the small-angle neutron scattering definition for the Flory effective interaction parameter χ_{eff}, the heat of mixing ΔH^{mix}, and the volume of mixing ΔV^{mix} are presented in the following paper, which focuses on the dependences of these properties on monomer structures, composition, pressure, interaction energies $\epsilon_{\mu\lambda}$, and molecular weights. The following paper primarily considers lower molecular weights, which are often studied for blends, while paper 4 will discuss the asymptotic high molecular weight limit. A detailed comparison of the LCT predictions with experimental data[2,16] for the PS/PVME blends as well as a further discussion on the influence of molecular structure and compressibility on χ_{eff}, ΔH^{mix}, and ΔV^{mix} is provided in paper 3, while a consideration of their influence on equations of state is presently in progress.

II. Packing Entropy for Multicomponent Compressible Polymer Systems in the Athermal Limit

To introduce the requisite notation, let $\mathbf{a}_\beta$, $\beta = 1, ..., z$ designate the vectors from a given lattice site to the z nearest-neighbor lattice sites, and let $\mathbf{r}_i$ denote the position of the ith lattice site with respect to the origin of coordinates. The condition that the lattice sites i and j are nearest neighbors is just

$$\mathbf{r}_i = \mathbf{r}_j + \mathbf{a}_\beta \tag{2.1}$$

for one of the possible bond directions $\beta = 1, ..., z$. Thus, this constraint may be imposed by using the Kronecker δ

$$\delta(i,j+\beta) \equiv \delta(\mathbf{r}_i,\mathbf{r}_j+\mathbf{a}_\beta) \tag{2.1a}$$

where the left-hand side of (2.1) provides a convenient shorthand notation.

The notation (2.1) is simply used to introduce the bonding constraints for the set of $\{n_\mu\}$ linear polymers of species μ with $N_\mu - 1$ bonds each. The first bond on the first chain of species μ enters into the counting scheme with the factor of

$$\sum_{i^\mu_{1_\mu,1_\mu},i^\mu_{2_\mu,1_\mu}} \sum_{\beta^\mu_{1_\mu,1_\mu}} \delta(i^\mu_{1_\mu,1_\mu},i^\mu_{2_\mu,1_\mu}+\beta^\mu_{1_\mu,1_\mu}) \equiv \sum_{i^\mu_{1,1},i^\mu_{2,1}} \sum_{\beta^\mu_{1,1}} \delta(i^\mu_{1,1},i^\mu_{2,1}+\beta^\mu_{1,1}) \tag{2.1b}$$

where the superscript labels the component number, the first subscript indicates the sequential monomer numbering along the chain ($1_\mu, ..., N_\mu$), the second one corresponds to the chain number of the given species ($1_\mu, ..., n_\mu$), and the bond in question may be in any of the z different possible orientations. The notation on the right-hand side of (2.1b) is used below to control the usual proliferation of the indexes required for describing multicomponent systems. The next bond in this chain has the obvious weight factor of $\sum_{i^\mu_{3,1}} \sum_{\beta^\mu_{2,1}} \delta(i^\mu_{2,1},i^\mu_{3,1} + \beta^\mu_{2,1})$ with the added excluded volume constraint between the nonbonded first and third monomers $i^\mu_{3,1} \neq i^\mu_{1,1}$, etc. This process is continued for all bonds and all chains. A factor of $(n_\mu!)^{-1}$ is introduced to account for the indistinguishability of all chains of a given species, and there is a symmetry number of $^1/_2$ for each chain. The partition function for packing a set of $\{n_\mu\}$ athermal monodisperse linear polymers of species $\mu = 1, 2, ..., k$ with polymerization indexes N_μ is thus written *exactly* as

$$W(\{n_\mu\},\{N_\mu\}) = \prod_{\mu=1}^{k} \frac{1}{n_\mu! 2^{n_\mu}} \times$$

$$\sum_{\substack{i^1_{1,1} \neq i^1_{2,1} \neq ... \neq i^1_{N_1,1} \\ \neq i^1_{1,2} \neq i^1_{2,2} \neq ... \neq i^1_{N_1,2} \\ ... \\ \neq i^1_{1,n_1} \neq i^1_{2,n_1} \neq ... \neq i^1_{N_1,n_1} \\ ... \\ \neq i^k_{1,n_k} \neq i^k_{2,n_k} \neq ... \neq i^k_{N_k,n_k}}} \prod_{m_\mu=1}^{n_\mu} \left\{ \prod_{\alpha_\mu=1}^{N_\mu-1} \sum_{\beta^\mu_{\alpha,m}=1}^{z} \delta(i^\mu_{\alpha,m},i^\mu_{\alpha+1,m}+\beta^\mu_{\alpha,m}) \right\} \tag{2.2}$$

where the notation of (2.1b) is used in which $y^\mu_{\alpha,m} \equiv y^\mu_{\alpha_\mu,m_\mu}$ ($y = i, \beta, ...$). The outside summation in (2.2) contains the excluded volume constraint that prohibits any two monomers from occupying the same lattice site. The excluded volume constraint $i^\mu_{\alpha,m} \neq i^\mu_{\alpha+1,m}$ between successively bonded monomers on a single chain is inserted into (2.2) for notational symmetry as the Kronecker δ function in (2.2) already prohibits bonded monomers from occupying the same lattice site. Equation 2.2 is an exact representation of the lattice model of a k-component compressible polymer mixture on a d-dimensional primitive Bravais lattice in the athermal limit. Solvent molecules are simply represented either as a single-site species with $N_\mu = 0$ or by dimers, trimers, etc., with $N_\mu = 1, 2, ...$, respectively. The treatment of nonprimitive Bravais lattices requires the use of more complicated bookkeeping, which is avoided here.

A. Mean Field Approximation. In order to extract the approximate Flory mean field contribution[1] from (2.2) and to enable the systematic computation of corrections, we first replace each Kronecker δ in (2.2) by its lattice Fourier transform

$$\delta(i,j+\beta) = N_l^{-1} \sum_{\mathbf{q}} \exp[i\mathbf{q}\cdot(\mathbf{r}_i - \mathbf{r}_j - \mathbf{a}_\beta)] \tag{2.3}$$

where N_l is the total number of lattice sites and the summation runs over the first Brillouin zone. The Kronecker δ from the α_μth bond on the m_μth chain of species μ in (2.2) introduces through (2.3) the wave vector summation index $\mathbf{q}^\mu_{\alpha_\mu,m_\mu} \equiv \mathbf{q}^\mu_{\alpha,m}$ for each bond. The cluster nature of the theory is made more apparent by first re-expressing (2.3) as

$$\sum_\beta \delta(i,j+\beta) = \frac{z}{N_l}\left\{1 + \frac{1}{z}\sum_{\mathbf{q}\neq 0} f(\mathbf{q}) \exp[i\mathbf{q}\cdot(\mathbf{r}_i - \mathbf{r}_j)]\right\} \tag{2.3a}$$

where the $\mathbf{q} = 0$ contribution from (2.3) emerges as the first term in braces on the right-hand side of (2.3a) and where $f(\mathbf{q})$ is the nearest-neighbor structure factor

$$f(\mathbf{q}) = \sum_{\beta=1}^{z} \exp(-i\mathbf{q}\cdot\mathbf{a}_\beta) \tag{2.4}$$

Substitution of (2.3a) into (2.2) converts the latter into another exact algebraic representation of the $\{n_\mu\}$ polymer

packing partition function

$$W(\{n_\mu\},\{N_\mu\}) = \prod_{\mu=1}^{k} \frac{1}{n_\mu! 2^{n_\mu}} \sum_{i_{1,1}^1 \neq \ldots \neq i_{N_k,n_k}^k} \prod_{m_\mu=1}^{n_\mu} \prod_{\alpha_\mu=1}^{N_\mu-1} \left[\frac{z}{N_l}\right] \times \left\{1 + \frac{1}{z} \sum_{\mathbf{q}_{\alpha,m}^\mu \neq 0} f(\mathbf{q}_{\alpha,m}^\mu) \exp[i\mathbf{q}_{\alpha,m}^\mu \cdot (\mathbf{r}_{i_{\alpha,m}^\mu} - \mathbf{r}_{i_{\alpha+1,m}^\mu})]\right\} \quad (2.5)$$

The product over the bond index α_μ and the chain index m_μ in (2.5) is of the form of a cluster expansion and bears strong similarity to Mayer's cluster expansion[9] for nonideal gases as follows: The lengthy expression 2.5 is represented more compactly by the notation

$$W(\{n_\mu\},\{N_\mu\}) = \prod_{\mu=1}^{k} \frac{1}{n_\mu! 2^{n_\mu}} \sum_{i_{1,1}^1 \neq \ldots \neq i_{N_k,n_k}^k} \prod_{m_\mu=1}^{n_\mu} \prod_{\alpha_\mu=1}^{N_\mu-1} \left\{\left[\frac{z}{N_l}\right][1 + X_{\alpha,m}^\mu]\right\} \quad (2.6a)$$

where the correlation corrections are defined for each polymer bond and are labeled by μ,α_μ, and m_μ as

$$X_{\alpha,m}^\mu \equiv X_{\alpha_\mu,m_\mu}^\mu = \frac{1}{z} \sum_{\mathbf{q}_{\alpha,m}^\mu \neq 0} f(\mathbf{q}_{\alpha,m}^\mu) \exp[i\mathbf{q}_{\alpha,m}^\mu \cdot (\mathbf{r}_{i_{\alpha,m}^\mu} - \mathbf{r}_{i_{\alpha+1,m}^\mu})] \quad (2.6b)$$

The wholly uncorrelated contribution stems from the factors of unity from *all bonds* in (2.6a) and yields the mean field approximation

$$W^{MF}(\{n_\mu\},\{N_\mu\}) = \prod_{\mu=1}^{k} \frac{1}{n_\mu! 2^{n_\mu}} \sum_{i_{1,1}^1 \neq \ldots \neq i_{N_k,n_k}^k} \prod_{m_\mu=1}^{n_\mu} \prod_{\alpha_\mu=1}^{N_\mu-1} \left[\frac{z}{N_l}\right] \quad (2.7)$$

Performing the excluded volume summation transforms (2.7) into

$$W^{MF}(\{n_\mu\},\{N_\mu\}) = \prod_{\mu=1}^{k} \frac{1}{n_\mu! 2^{n_\mu}} \frac{N_l!}{(N_l - \sum_{\mu=1}^{k} N_\mu n_\mu)!} \left[\frac{z}{N_l}\right]^{\sum_{\mu=1}^{k} n_\mu(N_\mu-1)} \quad (2.8)$$

which may be shown to recover the classic Flory–Huggins combinatorial packing entropy of mixing[1] for multicomponent compressible polymer systems in which immediate self-reversals are not omitted for convenience in the subsequent computations of correction terms below.

B. Cluster Expansion for Corrections to the Flory–Huggins Packing Entropy. The remaining terms in $\{X_{\alpha,m}^\mu\}$ of (2.6a) produce the corrections to the Flory–Huggins approximation. These corrections arise from local correlations in placing monomers or bonds on the lattice, correlations that are mathematically represented by the $X_{\alpha,m}^\mu$ and the excluded volume constraints. The $X_{\alpha,m}^\mu$ in (2.6) depend on the explicit positions of the two segments forming the α_μth bond on the m_μth polymer chain of type μ, and the complexity of evaluating contributions containing the $X_{\alpha,m}^\mu$ stems from the excluded volume constraints on these segment positions. Expanding the product in (2.6) naturally leads to the cluster expansion

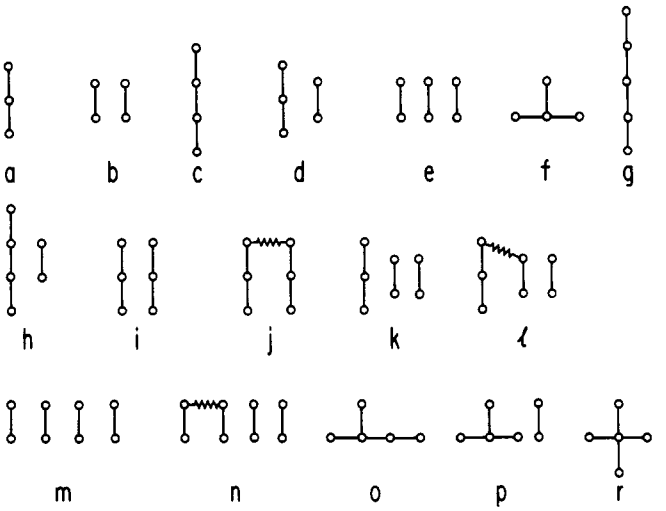

Figure 2. Athermal limit packing entropy diagram corrections to the mean field packing entropy (2.8) through order z^{-2}. This requires that the correlating bonds satisfy $B \leq 4$. Only contributions proportional to N_l are retained. The entropy diagrams are represented by vertices (circles) joined by correlating bonds (solid lines). Bonds lying nonsequentially on a single chain are connected by wiggly lines. The cumulant diagrams $[\gamma_D D_B]^{(c)}$ of eq 3.9 are constructed with diagrams a–r as the leading portions.[8]

$$\prod_{m_\mu=1}^{n_\mu} \prod_{\alpha_\mu=1}^{N_\mu-1} [1 + X_{\alpha,m}^\mu] = 1 + \sum_{\mu,\alpha_\mu,m_\mu} X_{\alpha,m}^\mu + \sum_{(\mu,\alpha_\mu,m_\mu)>(\mu',\alpha'_{\mu'},m'_{\mu'})} X_{\alpha,m}^\mu X_{\alpha',m'}^{\mu'} + \ldots \quad (2.9)$$

where the notation $(\mu,\alpha_\mu,m_\mu) > (\mu',\alpha'_{\mu'},m'_{\mu'})$ indicates that the summation in (2.9) runs over all distinct pairs of bonds in the system. The linear terms in $X_{\alpha,m}^\mu$ are called the one-bond contributions; the quadratic are the two-bond contributions, etc. When substituted into (2.6), the leading term of unity in (2.9) generates the Flory approximation of (2.8), while the remainder of (2.9) produces, respectively, the correlated one-bond, two-bond, etc., contributions to the cluster expansion for the packing entropy partition function

$$W(\{n_\mu\},\{N_\mu\}) = W^{MF}(\{n_\mu\},\{N_\mu\})\left\{1 + \frac{(N_l - \sum_{\mu=1}^{k} n_\mu N_\mu)!}{N_l!} \times \sum_{i_{1,1}^1 \neq \ldots \neq i_{N_k,n_k}^k} \left[\sum_{\mu,\alpha_\mu,m_\mu} X_{\alpha,m}^\mu + \sum_{(\mu,\alpha_\mu,m_\mu)>(\mu',\alpha'_{\mu'},m'_{\mu'})} X_{\alpha,m}^\mu X_{\alpha',m'}^{\mu'} + \ldots\right]\right\} \quad (2.10)$$

After some algebraic manipulations, the cluster expansion from (2.6) and (2.10) for athermal limit packing may be placed in one-to-one correspondence with that derived from the field theory formalism (when the latter is appropriately generalized to multicomponent compressible systems). In order to introduce the notation and concepts necessary for the new extensions in sections III and IV and in Appendix A, it is convenient now to describe briefly some additional steps in the derivation of the cluster expansion that enable the interested reader to use results from the previous field theory papers without the need to read or follow the field theory methods. Results of this

nature involve rules for the construction and evaluation of cluster diagrams and the definition of various counting indexes.

C. Diagrammatic Representation. Performing all summations in (2.10) leads to the much more compact notation and diagrammatic representation used by Nemirovsky et al.[8] Each correlating bond (i.e., factor of $X^{\mu}_{\alpha,m}$) is represented by a line connecting the bonded monomers. All contributing diagrams containing up to four correlating bonds are presented in Figure 2. Diagrams a and b of Figure 2 are the two-bond diagrams in which both bonds lie sequentially on the same chain and on two different chains, respectively. There is no two-bond diagram with nonsequential bonds belonging to one chain presented in Figure 2 because this contribution vanishes in the thermodynamic limit as does the one-bond correlation term. The value of an individual diagram with B bonds is written as the product of a monomer structure independent (but lattice structure dependent) connectivity factor D_B and a monomer structure dependent (but lattice structure independent) combinatorial factor γ_D. Using this notation converts eq 2.10 into the compact representation

$$W(\{n_\mu\},\{N_\mu\}) = W^{MF}(\{n_\mu\},\{N_\mu\})[1 + \sum_B \gamma_D(\{n_\mu\},\{N_\mu\})D_B] \tag{2.11}$$

where the sum over B designates both the sum over all diagrams with B bonds and the sum over B. We now summarize the definitions of γ_D and D_B in order to introduce necessary notation and new advances for generalization to multicomponent systems.

Figure 2 displays all the diagrams with up to $B = 4$ bonds that contribute to the packing entropy partition function for polymers of arbitrary architectures. Only diagrams a–e and g–n are appropriate for linear chains. A given diagram has B (correlating) bonds connecting N_v correlating monomers, which are called vertices. The connectivity factor D_B for each diagram with B bonds and N_v vertices is defined as

$$D_B = \frac{d_B}{N_l(N_l-1)...(N_l-N_v+1)} \tag{2.12}$$

where the expression in the denominator is just the number of ways of selecting the location of N_v distinguishable vertices from N_l lattice sites and where the factor d_B arises and is determined as follows: Label the vertices and $\mathbf{q}$ vectors associated with the bonds of a given diagram sequentially as i_1 through i_n and $\mathbf{q}_1$ through $\mathbf{q}_m$, respectively. Each bond δ contributes to d_B a factor of

$$b_\delta = \exp[i\mathbf{q}_\delta\cdot(\mathbf{r}_{i_\gamma} - \mathbf{r}_{i_{\gamma+1}})]f(\mathbf{q}_\delta)/z \tag{2.13}$$

that emerges from each $X^{\mu}_{\alpha,m}$ as in (2.6a). Summing the product of b_δ for all bonds of a diagram over all possible monomer positions (i.e., positions of vertices) and over the nonzero portion of the first Brillouin zone $\{\mathbf{q}_\delta \neq 0\}$ provides the definition of d_B as

$$d_B = \sum_{\mathbf{q}_1,...,\mathbf{q}_m\neq 0} \sum_{i_1\neq...\neq i_n} \prod_{\delta=1}^{m} b_\delta \tag{2.14}$$

Equation 2.14 may be simplified by use of the well-known lattice identity

$$\sum_j \exp(i\mathbf{q}\cdot\mathbf{r}_j) = N_l\,\delta_{\mathbf{q},0} \tag{2.15}$$

provided eq 2.14 is rewritten in terms of unrestricted summations over lattice sites. As described by Nemirovsky et al.,[8] this procedure can be represented in an equivalent diagrammatic form that corresponds to passing from the original diagrams d_B to a set of contracted diagrams $R_{B,c}$. The contraction process involves merging together sets of two or more vertices of diagrams d_B and therefore produces a new family of contracted diagrams. Contracted diagrams with vertices joined to others only by single lines have dangling ends and do not contribute to d_B. Consequently, their contributions can be omitted in the symbolic equation

$$d_B = \sum_c f^{(d)}_{B,c} R_{B,c} \tag{2.16}$$

where c is a sequential counting index for the contributing contracted diagrams and the coefficient $f^{(d)}_{B,c}$ is the product of a contraction factor of $\prod_{\lambda=1}^{N'_v}[(-1)^{k_\lambda-1}(k_\lambda-1)!]$ and the number of ways of forming a contracted diagram with N'_v vertices by contracting to single vertices k_1, k_2, ..., $k_{N'_v}$ distinguishable vertices of the original uncontracted diagram (note that $\sum_{\lambda=1}^{N'_v} k_\lambda = N_v$). The values of the contracted diagrams are lattice dependent, and their evaluation involves only summation over nonzero vectors $\{\mathbf{q}\}$ in an expression of the symbolic form

$$R_{B,c} = \sum_{\mathbf{q}_1,...,\mathbf{q}_B\neq 0} [N_l\delta(\sum\mathbf{q})]^{N'_v} \prod_{j=1}^{B} \frac{f(\mathbf{q}_j)}{z} \tag{2.17}$$

Each bond j of the contracted diagram $R_{B,c}$ has associated with it a wave vector $\mathbf{q}_j$ (or "momentum") and a factor of $f(\mathbf{q}_j)/z$. A momentum conservation condition $\sum\mathbf{q} = 0$ applies at each vertex of $R_{B,c}$. The complete list of diagrams $R_{B,c}$ and d_B contributing through order z^{-2} to the hypercubic lattice athermal limit packing entropy is displayed in ref 8 along with the values of the diagrams. Both $R_{B,c}$ and d_B are independent of the number of components in the system, so they remain the same as in ref 8, where more details of diagram evaluation and their contributions are provided.

While evaluation of diagrams $R_{B,c}$ and d_B proceeds identically for multicomponent and one-component systems, the monomer structure dependent combinatorial factor γ_D depends on the number of components. γ_D is defined as the number of ways of extracting the set of correlating bonds (displayed in B-bond diagram D_B) from all polymer chains in the system. For example, diagram e of Figure 2 contains three bonds, each lying on a different polymer. Hence, for a one-component system γ_D is obtained as $\gamma_D = N_1{}^3 n(n-1)(n-2)/3!$, where N_1 is the number of bonds in a single chain, n is number of chains in the system, and a factor 3! appears because of the indistinguishability of the three bonds on different chains of the same species. When applied to a binary blend, this counting produces γ_D with different values for four cases, shown in Chart I, where $N_1{}^{(\mu)}$ denotes the number of bonds in a single chain of species μ, and n_μ is the number of chains of species μ. The calculation of the combinatorial factors γ_D for a mixture requires the inclusion of all possible combinations in which each disconnected piece of a given diagram can belong to either component. The extension of the definition of γ_D to other diagrams of Figure 2 or to

Chart I

$$\gamma_D = \begin{cases} [N_1{}^{(1)}]^3 n_1(n_1-1)(n_1-2)/3!, & \text{three chains of species 1} \\ [N_1{}^{(2)}]^3 n_2(n_2-1)(n_2-1)/3!, & \text{three chains of species 2} \\ [N_1{}^{(1)}]^2 N_1{}^{(2)} n_1(n_1-1)n_2/2!, & \text{two chains of species 1 and one of species 2} \\ N_1{}^{(1)}[N_1{}^{(2)}]^2 n_1 n_2(n_2-1)/2!, & \text{one chain of species 1 and two of species 2} \end{cases}$$

multicomponent systems is rather straightforward. Reference 8 and Appendix B provide more details concerning the γ_D; our concern in this section is with the multicomponent generalization.

D. Packing Entropies. Packing entropies in the athermal limit are obtained from the Boltzmann definition

$$S(\{n_\mu\},\{N_\mu\}) = k \ln W(\{n_\mu\},\{N_\mu\}) = k \ln W^{MF}(\{n_\mu\},\{N_\mu\}) + k \ln [1 + \sum_B \gamma_D(\{n_\mu\},\{N_\mu\})D_B] \quad (2.18)$$

The product $\gamma_D D_B$ for diagrams of Figure 2 with disconnected pieces (i.e., with bonds on more than one chain) may contain contributions that vary as higher powers than N_l and are therefore unphysical. These hyperextensive terms are inherent to the lattice cluster expansion, but cancel exactly when the logarithm in the right-most term of (2.18) is expanded in a Taylor series and contributions are collected into cumulants.[17] The latter process leads to a new equation of the form

$$S(\{n_\mu\},\{N_\mu\}) = k \ln W^{MF}(\{n_\mu\},\{N_\mu\}) + k\sum_B [\gamma_D(\{n_\mu\},\{N_\mu\})D_B]^{(c)} \quad (2.19)$$

where $[\gamma_D D_B]^{(c)}$ represents the cumulant cluster diagram whose leading term involves the diagram with value $\gamma_D D_B$. The cumulant diagrams are described further in ref 5, and their sum in (2.19) produces directly the noncombinatorial packing entropy for athermal polymer systems.

III. Internal and Helmholtz Free Energies for Compressible Multicomponent Linear Polymer Mixtures

Interactions in polymer fluids involve both short-range repulsions and longer range attractions. The former are modeled by excluded volume constraints, presented in section II, while the latter are introduced by requiring that segments of species μ and λ interact with van der Waals attractive energies $\epsilon_{\mu\lambda}^{ij}$ that vanish unless i and j are nearest-neighbor lattice sites. The partition function then contains, in addition to the bonding and excluded volume constraints of section II, a Boltzmann factor for van der Waals interactions, which may be written for a multicomponent system in the equivalent forms

$$\exp[\sum_{\mu=1}^{k}\sum_{\lambda\le\mu}\sum_{\substack{i\in S_\mu\\ j\in S_\lambda}}{}'\epsilon_{\mu\lambda}^{ij}] = \prod_{\mu=1}^{k}\prod_{\lambda\le\mu}\prod_{\substack{i\in S_\mu\\ j\in S_\lambda}}{}'[1 + \sum_{\beta=1}^{z}\delta(i,j+\beta)f_{\mu\lambda}] \quad (3.1)$$

where $f_{\mu\lambda}$ is the Mayer f function

$$f_{\mu\lambda} = \exp(\epsilon_{\mu\lambda}) - 1 \quad (3.2)$$

associated with interactions between nearest-neighbor segments of species μ and λ, and S_μ designates the set of lattice sites occupied by polymer segments of species μ, etc. All energies $\epsilon_{\mu\lambda}$ are expressed in units of k_BT, and the prime on the sum and the product in (3.1) implies the constraint that when $\mu = \lambda$, we require $j \le i$. On the right-hand side of (3.1) we use Kronecker δ to represent explicitly the asumed nearest-neighbor character of the attractive interactions $\epsilon_{\mu\lambda}^{ij}$. The notation in (2.1a) which writes $\delta(i,j+\beta) = \delta(\mathbf{r}_i,\mathbf{r}_j+\mathbf{a}_\beta)$ is also applied to (3.1), but here the vector $\mathbf{a}_\beta$ designates the separation between a pair of interacting (neighboring) monomers. Extensions to nonnearest-neighbor interactions are possible but are excluded here for simplicity.

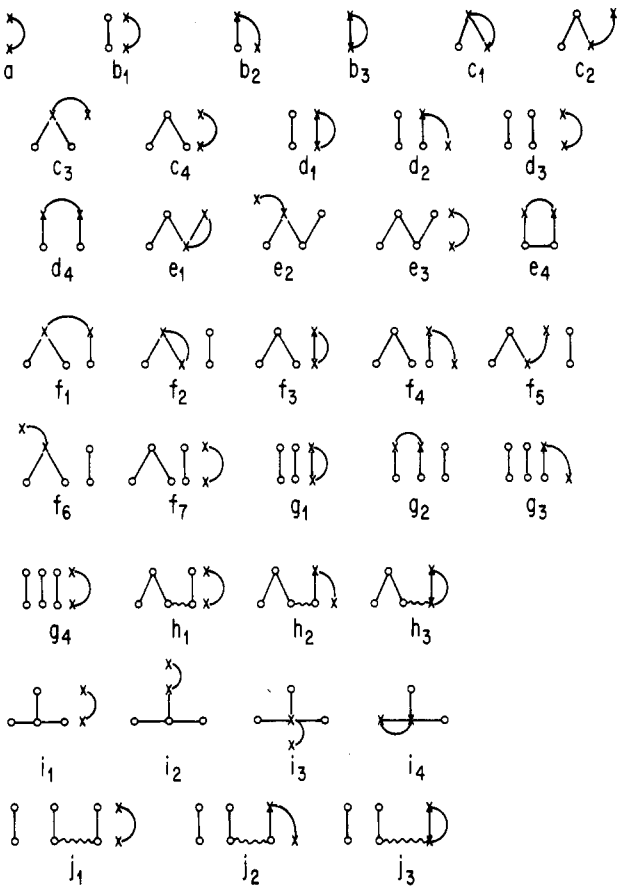

Figure 3. The first-order f-energy diagrams used to calculate energy corrections to FH mean field approximation through order z^{-2} and N_l. The l curved lines designate interactions between two bonded or nonbonded nearest-neighbor monomers (or portions thereof), and the straight lines represent the correlating bonds. Only diagrams for $B + l \le 4$ are required to the order indicated above.

The total configurational partition function $Z(\{n_\mu\},\{N_\mu\})$ for the interacting system is obtained by inserting the right-hand side of (3.1) into the summand on the right-hand side of (2.2), where the sets $\{S_\mu\}$ in (3.1) then correspond to the occupied sites listed in the summation indexes in (2.2). Thus, S_μ designates the set of lattice sites $i_{1,1}^\mu \ne \ldots \ne i_{N_\mu,n_\mu}^\mu$, and the exact total partition function is written compactly as

$$Z(\{n_\mu\},\{N_\mu\}) = \prod_{\mu=1}^{k}\frac{1}{n_\mu!2^{n_\mu}} \times \sum_{i_{1,1}^1 \ne \ldots \ne i_{N_k,n_k}^k}\prod_{m_\mu=1}^{n_\mu}\prod_{\alpha_\mu=1}^{N_\mu-1}\sum_{\beta_{\alpha,m}^\mu=1}^{z}\delta(i_{\alpha,m}^\mu, i_{\alpha+1,m}^\mu+\beta_{\alpha,m}^\mu) \times \exp[\sum_{\mu=1}^{k}\sum_{\lambda\le\mu}\sum_{\substack{i\in S_\mu\\ j\in S_\lambda}}{}'\epsilon_{\mu\lambda}^{ij}] \quad (3.3)$$

The sum over i and j in the exponent of (3.3) consequently runs over all pairs of lattice sites that are occupied by polymers. Hence, the summation indexes in the exponent portion of (3.3) are connected to the overall ones that also appear in the Kronecker δ of the "entropic factor" arising from (2.2).

The Helmholtz free energy $F(\{n_\mu\},\{N_\mu\})$ is obtained from the partition function $Z(\{n_\mu\},\{N_\mu\})$ through

$$F(\{n_\mu\},\{N_\mu\}) = -k_B T \ln Z(\{n_\mu\},\{N_\mu\}) \tag{3.4}$$

and all other thermodynamic properties may be evaluated from $F(\{n_\mu\},\{N_\mu\})$.

A. Mayer-like Cluster Expansion. The identity 2.3 may be applied to all Kronecker δ functions in $Z(\{n_\mu\},\{N_\mu\})$, and the entropic factor is therefore transformed as in (2.5). Along with this operation, the interaction energy in (3.1) is expanded in the usual Mayer cluster expansion

$$\prod_{\mu=1}^{k}\prod_{\lambda\le\mu}\prod_{\substack{i\in S_\mu\\ j\in S_\lambda}}{}' [1+\sum_{\beta=1}^{z}\delta(i,j+\beta)f_{\mu\lambda}] = 1 + \sum_{\mu=1}^{k}\sum_{\lambda\le\mu}\sum_{\beta=1}^{z}\sum_{i,j}{}' \delta(i,j+\beta)f_{\mu\lambda} + \sum_{\mu,\mu'=1}^{k}\sum_{\substack{\lambda\le\mu\\ \lambda'\le\mu'}}\sum_{\beta,\beta'=1}^{z}\sum_{(i,j)\neq(i',j')}{}'' \delta(i,j+\beta)\delta(i',j'+\beta')f_{\mu\lambda}f_{\mu'\lambda'} + \dots \tag{3.5}$$

Individual factors of $\delta(\dots)f$ in (3.5) are represented diagrammatically by curved interaction lines, running between neighboring lattice sites, to distinguish these interaction lines from the correlating bonds of section II. The diagrammatic representation of the partition function $Z(\{n_\mu\},\{N_\mu\})$ therefore contains both correlating bonds and interaction lines. When the identity (2.3a) is inserted into individual terms of the expansion 3.5, the interaction lines yield contributions from both the constant $\mathbf{q} = 0$ term of (2.3a) and from the $\mathbf{q} \neq 0$ correlations provided by the remaining part of (2.3a) containing $f(\mathbf{q})$. This appearance of $\mathbf{q} = 0$ contributions represents the main difference between correlating bonds and interaction lines, apart from slightly different counting rules, which are considerably simpler to derive from the expansion 3.5 than from the prior field theory formulation as discussed below.

Two previous papers[7,10] on incompressible polymer blends show that when large classes of contributions containing the $\mathbf{q} = 0$ parts from interaction lines are added together, the results vanish identically, leaving only the Flory–Huggins mean field energy as the nonzero residual from $\mathbf{q} = 0$ contributions. Considering the fact that an energy diagram with n interaction lines produces $n! - 1$ contributions from $\mathbf{q} = 0$ interaction lines, which must be evaluated individually, these $\mathbf{q} = 0$ portions represent the bulk of the computational labor as n grows. The previous finding that there is a complete vanishing of the sum of these contributions points to an underlying relation in the theory that we were unable to uncover within the original field theoretic formulation. However, this cancellation is readily proven by using the present algebraic representation. The proof is provided in Appendix A along with some counting rules for treating higher orders in the ϵ cluster expansion, rules that are greatly simplified by use of the algebraic formulation. Basically, the proof in Appendix A shows that $\mathbf{q} = 0$ contributions from the Kronecker δ in (3.5) may be ignored in all but the leading Flory–Huggins term, provided that each $\mathbf{q} \neq 0$ term is multiplied by the power series expansion of a simple explicit analytic function of the $\epsilon_{\mu\lambda}$.

After use of the theorem from Appendix A, the $\mathbf{q} \neq 0$ terms from all Kronecker δ in (3.5) provide the energy corrections to FH theory. The evaluation of these $\mathbf{q} \neq 0$ contributions follows just as for the athermal limit "entropy diagrams" with some modifications in the counting rules for the γ_D and some additional diagrams that have no counterpart for the athermal packing entropies.

B. Diagrammatic Representation. In analogy to the packing athermal limit entropy, the Helmholtz free energy (3.4) also has a diagrammatic representation, which may be written symbolically as

$$-\frac{F(\{n_\mu\},\{N_\mu\})}{k_B T} = \ln W^{MF}(\{n_\mu\},\{N_\mu\}) + N_l \frac{z}{2}\sum_{\mu=1}^{k}\sum_{\lambda=1}^{k} f_{\mu\lambda}\phi_\mu\phi_\lambda + \ln\{1 + \sum_{B,l}\gamma_{D,l}(\{n_\mu\},\{N_\mu\})D_{B,l}\} \tag{3.6}$$

where $W^{MF}(\{n_\mu\},\{N_\mu\})$ and $f_{\mu\lambda}$ are given by (2.11) and (3.2), respectively, and the quantities $D_{B,l}$ and $\gamma_{D,l}$ are generalizations of the D_B and γ_D of section II to a new class of diagrams that contain l f-interaction lines in addition to B correlating bonds. ϕ_i is the volume fraction of species i ($i = \mu, \lambda$), defined as $\phi_i = n_i M_i / N_l$; n_i denotes the number of chains of species i, M_i is the number of lattice sites occupied by a single chain, and N_l is the total number of lattice sites. The leading term from the expansion of the Mayer f function of the second term of the right-hand side of (3.6) in powers of $\epsilon_{\mu\lambda}$ provides the ($\mathbf{q} = 0$) Flory–Huggins approximation to the interaction energy. The higher terms in the former expansion give one simple set of corrections to the FH theory, while the last term in (3.6) yields the remaining corrections to the FH mean field approximation that arise from the $\mathbf{q} \neq 0$ entropy and energy diagrams. The sum over B and l in (3.6) denotes both a sum over all different diagrams with B bonds and l f-interaction lines and a sum over B and l, including $B = 0$ and $l = 0$ contributions (but not $B = l = 0$). Diagrams with two or more f-interaction lines connecting the same monomers are excluded as their values are more simply included by a power series expansion of $f_{\mu\lambda}$ factors (see Appendix A and (3.7) below). Diagrams with $l = 0$ and $B \neq 0$ are just the athermal limit entropy diagrams of Figure 2, while diagrams with $B = 0$ and $l \neq 0$ are the polymer structure independent energy diagrams having only f-interaction lines and are called the extended mean field terms by Bawendi and Freed.[6]

The f-interaction lines of the energy diagrams may be disconnected from or connected to any of B correlating bonds. Disconnected interaction lines correspond to interactions between two uncorrelated monomers. The ends of the interaction lines may be also singly or doubly connected to lines describing correlating segments as follows: Examples of diagrams with one f-interaction line and with up to $B = 3$ bonds are given in Figure 3, where crosses and circles are used to distinguish interacting from noninteracting monomers, respectively. Straight lines and curved ones designate correlating bonds and interaction lines, respectively. Only diagrams a–h and j of Figure 3 apply to linear polymer chains. The leading $\mathbf{q} = 0$ diagram a represents the FH term resulting from the interaction of two uncorrelated monomers. Diagrams b_1, b_2, and b_3 of Figure 3 are one-bond diagrams with, respectively, one disconnected interaction line, a singly connected line, and doubly connected line. These three main combinations appear also in the remaining first-order energy diagrams (of order $f_{\mu\lambda}$) of Figure 3. Examples of second-order energy diagrams (of order $f_{\mu\lambda}f_{\mu'\lambda'}$) with up to $B = 2$ bonds are provided in Figure 4. The first two diagrams of Figure 4 only contain f-interaction lines, which are connected sequentially (diagram a_1) and are disconnected (diagram a_2). Thus, the monomers in a_1 and a_2 are uncorrelated. Diagrams b_1–b_8, e_1–e_6, c_1–c_{13}, and d_1–d_{15} of Figure 4 also contain, respectively, one correlating bond, two correlating bonds lying sequentially on one chain, two bonds nonse-

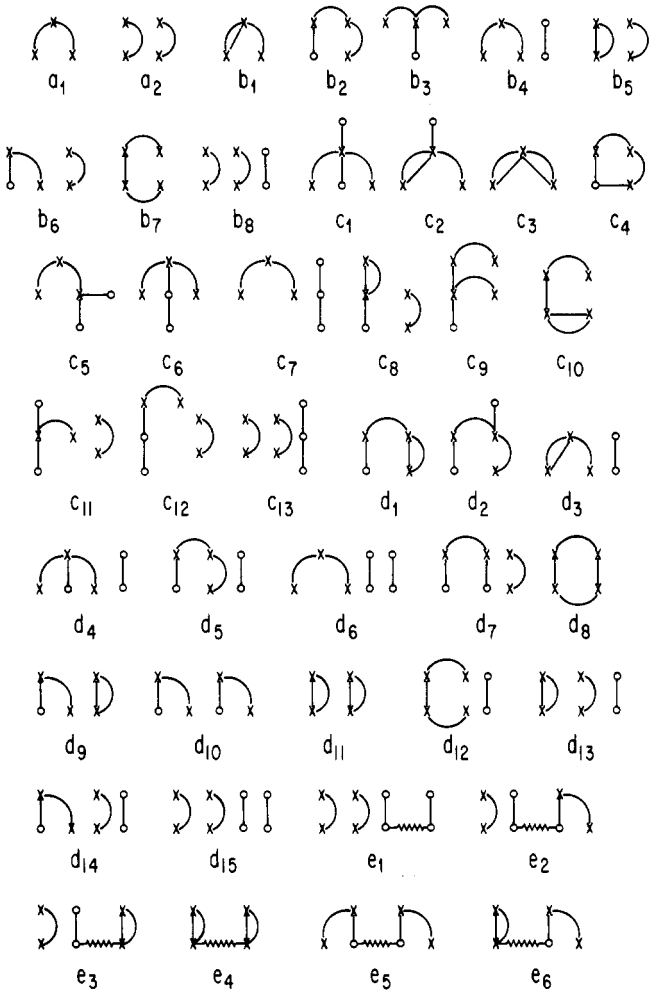

Figure 4. Same as Figure 3, but for the second-order f^2-energy diagrams through order z^{-1}.

quential on one chain, and two correlating bonds belonging to two different chains.

The generalized connectivity constant $D_{B,l}$ for a given diagram with B bonds and l interaction lines is determined as the product of the connectivity constant $D_{B'}$ for a corresponding entropy diagram with $B' = B + l$ bonds, formed by converting all interaction lines into correlating bonds, and a factor involving $f_{\mu\lambda}z/N_l$ for each of the l interaction lines

$$D_{B,l} = D_{B'=B+l}\left[\frac{f_{\mu\lambda}z/N_l}{1 + f_{\mu\lambda}\dfrac{z}{N_l}}\right]^l \tag{3.7}$$

where the indexes μ and λ generally differ for the l individual interaction lines and the denominator arises from elimination of the $\mathbf{q} = 0$ terms as described in Appendix A. When any of the l f-interaction lines connects a bonded pair of monomers in any of the B bonds, the equivalent entropy diagram $D_{B'}$ with $B' = B + l$ bonds does not exist. Examples are provided by diagrams b_3, c_1, ... in Figure 3. The evaluation of these additional $D_{B'}$ diagrams involves the same contraction process as for diagrams of Figure 2 and proceeds according to the rules (2.12–2.17) of section II. Each f-interaction line in a diagram $D_{B,l}$ is treated like a correlating bond contributing to $d_{B'}$ with the extra factor of $[f_{\mu\lambda}z/N_l]/[1 + (f_{\mu\lambda}z/N_l)]$.

C. Counting Rules. While the calculation rules for the monomer structure independent factors $D_{B,l}$ are almost identical for entropy and energy diagrams, the counting schemes for the monomer structure dependent combinatorial factors $\gamma_{D,l}$ are different. The generalized combinatorial factor $\gamma_{D,l}$ is defined as the product

$$\gamma_{D,l} = s_D\gamma_D \tag{3.8}$$

where γ_D is the number of ways of selecting the set of correlating bonds and uncorrelated interacting monomers (displayed in the diagram) from all polymer chains in the system, and s_D is the diagram symmetry number. In order to compute s_D for a given diagram, we begin by assigning species labels to all vertices on correlating bonds and to the interacting vertices that do not lie on correlating bonds, but the interaction lines are omitted. Then s_D is defined as the number of distinguishable ways of constructing the final diagram by connecting the interacting monomers with interaction lines. In this process all vertices are considered to be distinguishable, and the specification of species labels fixes the power of $\epsilon_{\mu\lambda}\epsilon_{\mu'\lambda'}$,... for the diagram with the given species labels. Examples are provided below and in Appendix C. A new feature of the combinatorial factor $\gamma_{D,l}$ lies in the appearance of the symmetry number, which reflects the relations between the summation over interacting pairs in the Mayer cluster expansion 3.5 and that over correlating bond positions in the excluded volume constraint of eq 3.3.

The field theory approach to the counting rules of s_D and γ_D is very complicated to derive for many diagrams of Figures 3 and 4. The present algebraic derivation proceeds directly from the Mayer cluster expansion in which s_D and γ_D emerge very simply. Consider for now a one-component system in which the interacting monomers are indistinguishable. Diagram a of Figure 3 has only one f-interaction line, and the number of ways of selecting the two monomers in this diagram is $\gamma_D = nM(nM - 1)/2!$, where n is the number of polymer chains, M is the number of lattice sites occupied by one chain, and a factor 2! arises because of the equivalence of the two indistinguishable interacting monomers. The symmetry number is $s_D = 1$ since diagram a does not contain any correlating bonds. Three different diagrams b_1, b_2, and b_3 appear in Figure 3 with one correlating bond and one f-interaction line. Diagram b_1 has the f-interaction line disconnected; hence, the interacting monomer position indexes differ from those associated with the correlating bond. Therefore, disconnected diagrams like b_1 always yield $s_D = 1$ while $\gamma_D = nN_1(nM-2)(nM-3)/2!$ for b_1, where N_1 denotes the number of bonds in one chain. The interaction line of diagram b_2 is singly connected with one end of the correlating bond. Thus, the interaction line and correlating bond can be connected at either end on the correlating bond, and there are two equivalent ways of drawing b_2 with distinguishable vertices. Hence, we have $s_D = 2$ for b_2. It also follows that $\gamma_D = nN_1(nM - 2)$ for b_2. The symmetry number for diagram b_3 is equal to unity since the two interacting monomers may be made coincident with the two bonded monomers only in one way. Diagram b_3 also has $\gamma_D = nN_1$. The calculation of γ_D for a binary system requires consideration of more combinations even for simple diagrams. Chart II provides examples for the diagrams a, b_1, b_2, and b_3 of Figure 3, where $N_1^{(\mu)}$ denotes the number of bonds in a single chain of species μ and n_μ is the number of chains of species μ. The calculation of γ_D for a polymer mixture involves labeling each unbonded monomer and each disconnected correlating bond or set of bonds as belonging to particular components. The computation of $\gamma_{D,l}$ for other diagrams of Figures 3 and 4 and for multicomponent systems is straightforward. The symmetry number s_D is independent of the number of components for diagrams a, b_1, b_2, and b_3 of Figure 3

Chart II

$$\gamma_a = \begin{cases} n_1 M_1 (n_1 M_1 - 1)/2!\,, & \text{two interacting monomers of species 1} \\ n_1 M_1 n_2 M_2\,, & \text{interacting monomers of species 1 and 2} \\ n_2 M_2 (n_2 M_2 - 1)/2!\,, & \text{two interacting monomers of species 2} \end{cases}$$

$$\gamma_{b_1} = \begin{cases} N_1^{(1)} n_1 (n_1 M_1 - 2)(n_1 M_1 - 3)/2!\,, & \text{bond and interacting monomers of species 1} \\ N_1^{(1)} n_1 n_2 M_2 (n_2 M_2 - 1)/2!\,, & \text{bond of species 1, interacting monomers of species 2} \\ N_1^{(1)} n_1 (n_1 M_1 - 2) n_2 M_2\,, & \text{bond of species 1, interacting monomers of species 1 and 2} \\ N_1^{(2)} n_2 (n_2 M_2 - 2)(n_2 M_2 - 3)/2!\,, & \text{bond and interacting monomers of species 2} \\ N_1^{(2)} n_2 n_1 M_1 (n_1 M_1 - 1)/2!\,, & \text{bond of species 2, interacting monomers of species 1} \\ N_1^{(2)} n_2 (n_2 M_2 - 2) n_1 M_1\,, & \text{bond of species 2, interacting monomers of species 1 and 2} \end{cases}$$

$$\gamma_{b_2} = \begin{cases} N_1^{(1)} n_1 (n_1 M_1 - 2)\,, & \text{bond and unbonded interacting monomer of species 1} \\ N_1^{(1)} n_1 n_2 M_2\,, & \text{bond of species 1, unbonded interacting monomer of species 2} \\ N_1^{(2)} n_2 (n_2 M_2 - 2)\,, & \text{bond and unbonded interacting monomer of species 2} \\ N_1^{(2)} n_2 n_1 M_1\,, & \text{bond of species 2, unbonded interacting monomer of species 1} \end{cases}$$

$$\gamma_{b_3} = \begin{cases} N_1^{(1)} n_1\,, & \text{correlating bond of species 1} \\ N_1^{(2)} n_2\,, & \text{correlating bond of species 2} \end{cases}$$

because they contain only one correlating bond. However, when there are correlating bonds on more than one chain, as in diagrams of classes d, f, g, and j of Figure 3, then s_D becomes dependent on the number of components. More details on the evaluation of γ_D and for calculation of s_D are presented in Appendix C.

D. Thermodynamic Properties. The procedure for expressing the Helmholtz free energy as a direct sum of diagrammatic contributions involves the expansion of each Mayer f function $f_{\mu\lambda}$ of (3.6) in a power series in $\epsilon_{\mu\lambda}$ and the subsequent expansion of the last term of (3.6) in a Taylor series. The resulting contributions with a given power of $\epsilon_{\mu\lambda}$ are collected into cumulants. This process ensures that individual diagram contributions proportional to higher than the first power of N_l cancel and that the free energy is extensive (i.e., linear in N_l) in the thermodynamic limit. We represent the result as

$$-\frac{F(\{n_\mu\},\{N_\mu\})}{k_B T} = \ln W^{\mathrm{MF}}(\{n_\mu\},\{N_\mu\}) + N_l \frac{z}{2}\sum_{\mu=1}^{k}\sum_{\lambda=1}^{k}\epsilon_{\mu\lambda}\phi_\mu\phi_\lambda + \sum_{B,l}[\gamma_{D,l}(\{n_\mu\},\{N_\mu\})D_{B,l}]^{(c)} \quad (3.9)$$

where $[\gamma_{D,l}(\{n_\mu\},\{N_\mu\})D_{B,l}]^{(c)}$ are the generalized cumulant cluster diagrams, which reduce for $l = 0$ to the cumulant cluster diagrams of section III. The sum of the generalized cumulant cluster diagrams provides all corrections to FH, while the two first terms on the right-hand side of (3.9) are the $\mathbf{q} = 0$ FH athermal entropic and energetic contributions, respectively.

As noted above, the algebraic formulation leads to the theorem of Appendix A; this theorem considerably reduces the computational labor from that required by the field theory formalism. For example, the latter approach yields contributions in $\epsilon^2 z^2$, whose sum vanishes identically, while such terms can be eliminated at the outset with the results of Appendix A. Likewise, this theorem also eliminates all contributions in $\epsilon^3 z^3$, $\epsilon^3 z^2$, $\epsilon^4 z^3$ and $\epsilon^4 z^2$ that previously would be cancelled only by consideration of many diagrams. These simplifications become even more significant in applications to compressible systems.

IV. Generalization of the Lattice Cluster Theory to Compressible Multicomponent Mixtures for Polymers with Arbitrary Architectures and Structured Monomers

The actual polymer molecular structure is represented more faithfully by models in which individual monomers are allowed to occupy several neighboring lattice sites as dictated by their molecular architectures. This leads us to a consideration of structured polymer chains, examples of which are given by the sequential bonding of extended monomers, such as those depicted in b–e of Figure 1 for short chains with $N_\mu - 1 = 6$ backbone bonds in each case. A wide range of vinyl monomer structures will be considered in paper 3.

A. Athermal Limit Packing Entropies. The analysis for athermal limit packing entropies proceeds simply by introducing Kronecker δ for each bond and overall excluded volume constraints on all occupied lattice sites. Complexities appear due to the bookkeeping required for indexes associated with the lattice sites occupied by the side groups. To simplify matters, we illustrate the generalization using an example in which all chains have the structure given by type b of Figure 1, as more general cases follow similarly. This system contains $\{n_\mu\}$ chains of species $\mu = 1, 2, \ldots, k$, where a single chain of species μ has $N_\mu - 1$ backbone bonds and $N_\mu - 2$ side bonds. The exact packing partition function $W(\{n_\mu\},\{N_\mu\})$ has the form of eq 2.2, with the excluded volume constraints extended to cover

the lattice sites occupied by the side bonds

$$W(\{n_\mu\},\{N_\mu\}) = \prod_{\mu=1}^{k} \frac{1}{n_\mu! 2^{n_\mu}} \times \sum_{\substack{i_{1,1}^1 \neq \ldots \neq i_{N_k,n_k}^k \\ \neq j_{1,1}^1 \neq \ldots \neq j_{N_k-2,n_k}^k}} \prod_{m_\mu=1}^{n_\mu} \{ \prod_{\alpha_\mu=1}^{N_\mu-1} \sum_{\beta_{\alpha,m}^\mu=1}^{z} \delta(i_{\alpha,m}^\mu, i_{\alpha+1,m}^\mu + \beta_{\alpha,m}^\mu) \times \prod_{\omega_\mu=1}^{N_\mu-2} \sum_{\beta_{\omega,m}^\mu=1}^{z} \delta(i_{\omega,m}^\mu, j_{\omega,m}^\mu + \beta_{\omega,m}^\mu) \quad (4.1)$$

where $j_{\omega,m}^\mu$ designates the position of the lattice site occupied by the side group portion of a monomer of polymer with architecture b and the indexes α and ω label the backbone and side group bonds, respectively. The extension of (4.1) to other chain architectures is straightforward and only requires the addition (or deletion) of Kronecker δ for side group bonds and the specification of indexes for any additional side group bonds in the excluded volume constraints on the summation in (4.1).

Using (2.3a) of section II converts (4.1) into

$$W(\{n_\mu\},\{N_\mu\}) = \prod_{\mu=1}^{k} \frac{1}{n_\mu! 2^{n_\mu}} \times \sum_{\substack{i_{1,1}^1 \neq \ldots \neq i_{N_k,n_k}^k \\ \neq j_{1,1}^1 \neq \ldots \neq j_{N_k-2,n_k}^k}} \prod_{m_\mu=1}^{n_\mu} \{ \prod_{\alpha_\mu=1}^{N_\mu-1} [\frac{z}{N_l}(1 + X_{\alpha,m}^\mu)] \times \prod_{\omega_\mu=1}^{N_\mu-2} [\frac{z}{N_l}(1 + X_{\omega,m}^\mu)] \} \quad (4.2)$$

with the correlating bond corrections defined for each backbone bond labeled by μ, α_μ, and m_μ as

$$X_{\alpha,m}^\mu \equiv X_{\alpha_\mu,m_\mu}^\mu = \frac{1}{z} \sum_{\mathbf{q}_{\alpha,m}^\mu \neq 0} f(\mathbf{q}_{\alpha,m}^\mu) \exp[i\mathbf{q}_{\alpha,m}^\mu \cdot (\mathbf{r}_{i_{\alpha,m}^\mu} - \mathbf{r}_{i_{\alpha+1,m}^\mu})] \quad (4.2a)$$

while each side group bond labeled by μ, ω_μ, and m_μ has the correction term

$$X_{\omega,m}^\mu \equiv X_{\omega_\mu,m_\mu}^\mu = \frac{1}{z} \sum_{\mathbf{q}_{\omega,m}^\mu \neq 0} f(\mathbf{q}_{\omega,m}^\mu) \exp[i\mathbf{q}_{\omega,m}^\mu \cdot (\mathbf{r}_{i_{\omega,m}^\mu} - \mathbf{r}_{j_{\omega,m}^\mu})] \quad (4.2b)$$

The mean field FH approximation is again obtained from the factors of unity from all bonds in (4.2)

$$W^{MF}(\{n_\mu\},\{N_\mu\}) = \prod_{\mu=1}^{k} \frac{1}{n_\mu! 2^{n_\mu}} \times \sum_{i_{1,1}^1 \neq \ldots \neq i_{2N_k-2,n_k}^k} \prod_{m_\mu=1}^{n_\mu} \prod_{\xi_\mu=1}^{2N_\mu-3} [\frac{z}{N_l}] \quad (4.3)$$

$$= \prod_{\mu=1}^{k} \frac{1}{n_\mu! 2^{n_\mu}} \frac{N_l!}{[N_l - \sum_{\mu=1}^{k} M_\mu n_\mu]!} \times [\frac{z}{N_l}]^{\sum_{\mu=1}^{k}(M_\mu-1)n_\mu} \quad (4.3a)$$

and does not distinguish between backbone and side group bonds as (4.3a) is equivalent to (2.8) when the former is written in terms of the number of lattice sites $M_\mu = 2(N_\mu - 1)$ covered by a chain of species μ with architecture of type b. The index ξ_μ in (4.3) runs over all bonds.

Expanding the products in (4.2) recovers a cluster expansion identical in form with (2.9), derived in section II for linear polymers

Table I
Values of "Entropy" Diagrams Contributing to the Athermal Packing Entropy per Site through Order z^{-2} for k-Component Polymer Mixture[a]

diagram of Figure 2	contribution from cumulant diagram
a	$C_1^{(s)} = -\frac{1}{z}\sum_{\kappa=1}^{k} N(2,\kappa)\phi_\kappa$
b	$C_2^{(s)} = \frac{1}{z}\sum_{\kappa=1}^{k}\sum_{\lambda=1}^{k} N(1,\kappa)N(1,\lambda)\phi_\kappa\phi_\lambda$
c	$C_3^{(s)} = \frac{1}{z^2}\sum_{\kappa=1}^{k} N(3,\kappa)\phi_\kappa$
d	$C_4^{(s)} = -\frac{4}{z^2}\sum_{\kappa=1}^{k}\sum_{\lambda=1}^{k} N(1,\kappa)N(2,\lambda)\phi_\kappa\phi_\lambda$
e	$C_5^{(s)} = \frac{8}{3z^2}\sum_{\kappa=1}^{k}\sum_{\lambda=1}^{k}\sum_{\mu=1}^{k} N(1,\kappa)N(1,\lambda)N(1,\mu)\phi_\kappa\phi_\lambda\phi_\mu$
f	$C_6^{(s)} = \frac{2}{z^2}\sum_{\kappa=1}^{k} N(\perp,\kappa)\phi_\kappa$
g	$C_7^{(s)} = 0$
h	$C_8^{(s)} = -\frac{2}{z^2}\sum_{\kappa=1}^{k}\sum_{\lambda=1}^{k} N(1,\kappa)N(3,\lambda)\phi_\kappa\phi_\lambda$
i	$C_9^{(s)} = \frac{1}{z^2}\sum_{\kappa=1}^{k}\sum_{\lambda=1}^{k} N(2,\kappa)N(2,\lambda)\phi_\kappa\phi_\lambda - \frac{1}{2z^2}\sum_{\kappa=1}^{k}[N(2,\kappa)]^2 M_\kappa\phi_\kappa$
j	$C_{10}^{(s)} = \frac{1}{z^2}\sum_{\kappa=1}^{k} N(2,2;\kappa)\phi_\kappa$
k	$C_{11}^{(s)} = \frac{2}{z^2}\sum_{\kappa=1}^{k}\sum_{\lambda=1}^{k} N(1,\kappa)N(1,\lambda)N(2,\lambda)M_\lambda\phi_\kappa\phi_\lambda$
l	$C_{12}^{(s)} = -\frac{2}{z^2}\sum_{\kappa=1}^{k}\sum_{\lambda=1}^{k} N(1,\kappa)N(1,2;\lambda)\phi_\kappa\phi_\lambda$
m	$C_{13}^{(s)} = \frac{2}{z^2}\sum_{\kappa=1}^{k}\sum_{\lambda=1}^{k}\sum_{\mu=1}^{k}\sum_{\eta=1}^{k} N(1,\kappa) \times N(1,\lambda)N(1,\mu)N(1,\eta)\phi_\kappa\phi_\lambda\phi_\mu\phi_\eta - \frac{2}{z^2}\sum_{\kappa=1}^{k}\sum_{\lambda=1}^{k}\sum_{\mu=1}^{k}[N(1,\kappa)]^2 N(1,\lambda)N(1,\mu)M_\kappa\phi_\kappa\phi_\lambda\phi_\mu$
n	$C_{14}^{(s)} = \frac{4}{z^2}\sum_{\kappa=1}^{k}\sum_{\lambda=1}^{k}\sum_{\mu=1}^{k} N(1,1;\kappa)N(1,\lambda)N(1,\mu)\phi_\kappa\phi_\lambda\phi_\mu$
o	$C_{15}^{(s)} = \frac{1}{z^2}\sum_{\kappa=1}^{k} N(\perp',\kappa)\phi_\kappa$
p	$C_{16}^{(s)} = -\frac{6}{z^2}\sum_{\kappa=1}^{k}\sum_{\lambda=1}^{k} N(1,\kappa)N(\perp,\lambda)\phi_\kappa\phi_\lambda$
r	$C_{17}^{(s)} = \frac{3}{z^2}\sum_{\kappa=1}^{k} N(+,\kappa)\phi_\kappa$

[a] $N(i,\alpha) \equiv N_i^{(\alpha)}/M_\alpha$, $\alpha = 1, 2, \ldots, k$; $N(i,j;\alpha) \equiv N_{ij}^{(\alpha)}/M_\alpha$, $\alpha = 1, 2, \ldots, k$; $\phi_\alpha = n_\alpha M_\alpha/N_l$, $\alpha = 1, 2, \ldots, k$; $\sum_{\alpha=1}^{k}\phi_\alpha + \phi_v = 1$.

$$\prod_{m_\mu=1}^{n_\mu}\prod_{\alpha_\mu=1}^{N_\mu-1}\prod_{\omega_\mu=1}^{N_\mu-2}[1+X^\mu_{\alpha,m}][1+X^\mu_{\omega,m}] =$$

$$1+\sum_{\mu,\alpha_\mu,m_\mu}X^\mu_{\alpha,m}+\sum_{\mu,\omega_\mu,m_\mu}X^\mu_{\omega,m}+$$

$$\sum_{(\mu,\alpha_\mu,m_\mu)>(\mu',\alpha'_{\mu'},m'_{\mu'})}X^\mu_{\alpha,m}X^{\mu'}_{\alpha',m'}+\sum_{(\mu,\omega_\mu,m_\mu)>(\mu',\omega'_{\mu'},m'_{\mu'})}X^\mu_{\omega,m}X^{\mu'}_{\omega',m'}+$$

$$\sum_{\mu,\mu',\alpha_\mu,\omega_{\mu'},m_\mu,m_{\mu'}}X^\mu_{\alpha,m}X^{\mu'}_{\omega,m'}+\dots \quad (4.4a)$$

$$=1+\sum_{\mu,\xi_\mu,m_\mu}X^\mu_{\xi,m}+\sum_{(\mu,\xi_\mu,m_\mu)>(\mu',\xi'_{\mu'},m'_{\mu'})}X^\mu_{\xi,m}X^{\mu'}_{\xi',m'}+\dots \quad (4.4b)$$

where the notation $(\mu, \alpha_\mu, m_\mu) > (\mu', \alpha'_{\mu'}, m'_{\mu'})$, $(\mu, \omega_\mu, m_\mu) > (\mu', \omega'_{\mu'}, m'_{\mu'})$, and $(\mu, \xi_\mu, m_\mu) > (\mu', \xi'_{\mu'}, m'_{\mu'})$ designates that summations in (4.4a) and (4.4b) run, respectively, over all distinct pairs of backbone bonds, side group bonds, and all types of bonds. The notation $\mu,\mu',\alpha_\mu,\omega_{\mu'},m_\mu,m_{\mu'}$ implies that one bond belongs to the backbone and the other to a side group. Equation 4.4b has a form that is identical with that of (2.9), and this occurs also for other monomer structures when (4.4b) is merely written in terms of summations over all bonds of all types.

Equation 4.2 can be rewritten following (2.10) as the product of the mean field contribution $W^{MF}(\{n_\mu\},\{N_\mu\})$ and successive corrections to $W^{MF}(\{n_\mu\}\{N_\mu\})$

$$W(\{n_\mu\},\{N_\mu\}) = W^{MF}(\{n_\mu\},\{N_\mu\})\Bigg\{1+\frac{[N_l-\sum_{\mu=1}^{k}M_\mu n_\mu]!}{N_l!}\times$$

$$\sum_{i^1_{1,1}\neq\dots\neq i^k_{2N_k-2,n_k}}\Big[\sum_{\mu,\xi_\mu,m_\mu}X^\mu_{\xi,m}+$$

$$\sum_{(\mu,\xi_\mu,m_\mu)>(\mu',\xi'_{\mu'},m'_{\mu'})}X^\mu_{\xi,m}X^{\mu'}_{\xi',m'}+\dots\Big]\Bigg\} \quad (4.5)$$

Performing all summations in (4.5) and introducing the diagrammatic quantities γ_D and D_B transform eq 4.5 into eq 2.11 of section II

$$W(\{n_\mu\},\{N_\mu\}) = W^{MF}(\{n_\mu\},\{N_\mu\})[1+\sum_B\gamma_D(\{n_\mu\},\{N_\mu\})D_B] \quad (4.6)$$

Polymer structure is involved only in the combinatorial factors γ_D, while the diagram connectivity constants D_B depend only on the topology of the B bonds on the given lattice and not on monomer internal structure. Since the sum in (4.6) denotes a sum over all diagrams with B bonds and over B, new branched diagrams appear (such as diagrams f and o in Figure 2) that are absent for linear polymers. Thus, the only new feature arising from introducing monomer structures is the appearance of more diagrams and new counting indexes for the γ_D as discussed below.

Finally, the form in (4.5) describes adequately a mixture of polymers with different chain architectures when the $2(N_\mu - 1)$ in the mean field portion is replaced by the number of lattice sites M_μ occupied by a chain of species μ and when the excluded volume constraints are extended to all lattice sites occupied by the backbone and side groups. Diagrams are constructed and evaluated along the rules of section II, and contributions from each disconnected piece of the diagrams in Figure 2 belonging to either component μ are summed together.

The packing entropy calculations are performed here to order z^{-2}, which involves the retention of all diagrams having up to $B = 4$ bonds. This yields an equation identical with eq 2.19 but with additional diagrams included in the sum. According to this equation, the athermal limit packing entropy for a multicomponent structured polymer mixture is the sum of the mean field FH entropic contribution s^{MF} and successive entropic corrections represented by the cumulant cluster diagram contributions $C_j^{(s)} \equiv (1/N_l)[\gamma_D(\{n_\mu\},\{N_\mu\})D_B]^{(c)}$ with a convenient sequential counting index j

$$\frac{S_\infty(\{n_\mu\},\{N_\mu\})}{N_l k_B} = s^{MF}+\sum_{j=1}C_j^{(s)} \quad (4.7)$$

The mean field specific entropy (per site) s^{MF} follows from eq 4.3a as

$$s^{MF} = -\phi_v\ln\phi_v-\sum_{\mu=1}^{k}\frac{\phi_\mu}{M_\mu}\Big[\ln\phi_\mu+\ln\frac{2z}{M_\mu}-1-M_\mu\ln z+M_\mu\Big] \quad (4.8)$$

where ϕ_v denotes the void volume fraction, M_μ is defined above as the number of lattice sites occupied by a single chain of species μ, and z is the lattice coordination number.

The cumulant entropic corrections to s^{MF} are provided in Table I, where the first column specifies the leading diagrams from Figure 2 for which the cumulant cluster diagrams $[\gamma_D D_B]^{(c)}$ are constructed. In order to conform to the notation of Nemirovsky et al.[8] for structured monomers, the chains are taken to have N_μ bonds along the chain backbone and to cover M_μ lattice sites per chain. The structure dependences in Table I enter through the combinatorial numbers $N_B^{(\mu)}$ that specify the architecture of species μ. Values of $N_B^{(\mu)}$ for polymers with structures a–c in Figure 1 are presented in Table I of Nemirovsky et al.,[8] while the generalization to other architectures is provided by the following definitions: $N_i^{(\mu)}$ is the number of sequentially bonded sets of i bonds (from main-chain and/or side groups) in a single polymer chain of species μ that covers M_μ sites; $N_{i,j}^{(\mu)}$ is the number of nonsequentially bonded sets of i and j sequential bonds; $N_\perp^{(\mu)}$ and $N_+^{(\mu)}$ are the numbers of ways in which three and four bonds meet at a lattice site, respectively, and $N_{\perp'}^{(\mu)}$ is the number of four bond sets depicted in diagram o of Figure 2. (The definitions of $N_{i,j}^{(\mu)}$ in ref 8 do not include the symmetry number 1/2!, which is, however, properly included in the calculated entropies of that paper and which is absorbed here into the definition of the $N_{i,i}^{(\mu)}$ to account for the indistinguishability of two identical bonds.) These structure-specific combinatorial indexes are readily evaluated for polymers (or solvent molecules) with regular repeating or rather irregular architectures. A future paper will give $N_B^{(\mu)}$ for a large number of different vinyl monomer structures.

The athermal limit entropies of mixing ΔS_∞^{mix} may be obtained from (4.7) by subtracting $\sum_\mu\phi_\mu s_\mu$, where $s_\mu = s_\mu(\phi_\mu = 1)$ is the specific entropy (per site) of pure component μ at unit volume fraction ϕ_μ that is obtained from Nemirovsky et al.[8] with a minor correction.[18]

B. Helmholtz Free Energy. Introducing interaction energies into the partition function for a mixture of polymers with structured monomers proceeds identically with the scheme described by eqs 3.1–3.9 of section III for linear polymer systems, provided that the side and backbone groups interact with the same energies. The inclusion of different interaction energies for backbone and side groups requires the definition of new counting indexes $N_B^{(\omega)}$ and more tedious bookkeeping, but it follows directly. If, for example, there are three independent sets of interaction energies $\epsilon_{\mu\lambda}^{\alpha\alpha}$, $\epsilon_{\mu\lambda}^{\omega\omega}$, and $\epsilon_{\mu\lambda}^{\alpha\omega}$ (where indexes α and ω are related to backbone and side groups, respectively), it is necessary to evaluate the correlation corrections $X_{\alpha,m}^{\mu}$, $X_{\omega,m}^{\mu}$, ... in the cluster expansion 4.4 for each $\epsilon_{\mu\lambda}^{ij}$ separately, and this is quite cumbersome even for diagrams with one f-interaction line. Therefore, for simplicity, the computations here are performed for polymer chains with energetically equivalent side and backbone groups for each species.

The diagrammatic representation of the Helmholtz free energy $F(\{n_\mu\},\{N_\mu\})$ contains the energy diagrams obtained by expanding the Mayer f function $f_{\mu\lambda}$ of (3.6) in a power series in $\epsilon_{\mu\lambda}$. Diagrams with the lowest order contribution of the nth power of $\epsilon_{\mu\lambda}$ are called n-order energy diagrams. Polymers having structured monomers contribute to the diagrammatic expansion of the free energy $F(\{n_\mu\},\{N_\mu\})$ new energy diagrams (such as diagrams i_1–i_4 in Figure 3), which do not appear for linear polymer systems.

The validity of eq 3.9 for a mixture of polymers with different molecular architectures requires that the summation indexes for the B correlating bonds and l interaction lines run over all components, all numbers of bonds and interaction lines, and all diagrams (excluding diagrams with multiple interaction lines connecting a pair of lattice sites). Since a comparison of the LCT with Monte Carlo simulations for the linear polymer–monomer solvent system indicates that higher order energy terms are numerically insignificant beyond ϵ^2 for the one-phase region and coexistence curve, the present calculations of multicomponent energy diagrams are confined to diagrams with up to $l = 2$ f-interaction lines and up to $B' \equiv B + l = 4$. This maintains the correspondence with the athermal limit packing entropy diagrams of section II having up to $B = 4$ bonds. Thus, we retain the first-order energy corrections up to order z^{-2} for the leading FH interaction energy and the second-order energy corrections through order z^{-1} to the leading extended mean field (EMF) term. The EMF interaction energy is defined as energetic contributions arising from interactions of uncorrelated monomers; the first EMF term corresponds to interactions between two monomer pairs, is order of ϵ^2, and emerges from diagrams a_1 and a_2 of Figure 4. The specific Helmholtz free energy (3.9) can be rewritten as

$$-\frac{F(\{n_\mu\},\{N_\mu\})}{N_l k_B T} = \frac{S_\infty(\{n_\mu\},\{N_\mu\})}{N_l k_B} + \sum_{j=0} C_j^{(\epsilon)} + \sum_{j=0} C_j'^{(\epsilon^2)} + \sum_{j=1} C_j^{(\epsilon^2)} \quad (4.9)$$

where $S_\infty(\{n_\mu\},\{N_\mu\})$ is the athermal limit packing entropy (4.7), and the cumulant cluster energy diagram contributions $C_j^{(\epsilon)}$, $C_j'^{(\epsilon^2)}$, and $C_j^{(\epsilon^2)}$ are labeled by the sequential index j and are defined by

$$C_j^{(\epsilon)} \equiv \frac{1}{N_l}[\gamma_{D,1}(\{n_\mu\},\{N_\mu\})D_{B,1}^{(\epsilon)}]^{(c)}$$

$$C_j'^{(\epsilon^2)} \equiv \frac{1}{N_l}[\gamma_{D,1}(\{n_\mu\},\{N_\mu\})D_{B,1}^{(\epsilon^2)}]^{(c)}$$

$$C_j^{(\epsilon^2)} \equiv \frac{1}{N_l}[\gamma_{D,2}(\{n_\mu\},\{N_\mu\})D_{B,2}^{(\epsilon^2)}]^{(c)} \quad (4.10)$$

with $D_{B,l}^{(\epsilon^n)}$ denoting the ϵ^n-order portion of $D_{B,l}$ (after the expansion of the Mayer f functions in (3.7) in a Taylor series in ϵ).

The contributions $C_0^{(\epsilon)}$ and $C_1^{(\epsilon^2)}$ in (4.9) are the FH and second-order EMF interaction energies, respectively, that are independent of monomer structure and chain connectivity. In the present calculations, which retain $B' \leq 4$, only the first four diagrams of Figure 3 contribute to $F(\{n_\mu\},\{N_\mu\})$ in the second order of ϵ. Energy corrections of order ϵ^3 and ϵ^4 are found to be numerically irrelevant, and therefore, they are omitted here. The first-order energy corrections $C_j^{(\epsilon)}$ ($j \geq 1$) to the FH energy ($C_0^{(\epsilon)}$) are provided in Table II, where the first column shows the leading diagram of the cumulant cluster diagram $[\gamma_{D,1}(\{n_\mu\},\{N_\mu\})D_{B,1}]^{(c)}$. Table II also presents the second-order corrections $C_j'^{(\epsilon^2)}$, which arise simply from the expansion of the Mayer f functions in (3.6). (Note that in the field theory formulation of the LCT their evaluation requires the computation of additional diagrams.) The remaining part of the second-order energetic corrections $C_j^{(\epsilon^2)}$ is collected in Table III, where the first column specifies the leading diagrams $D_{B,2}$ of the cumulant cluster diagrams $[\gamma_{D,2}(\{n_\mu\},\{N_\mu\})D_{B,2}]^{(c)}$. The expressions in Tables I–III also correct some previous results[7] for an incompressible binary blend. The free energy of mixing may be calculated from eq 4.9 by subtracting $\sum_{\mu=1}^{k}\phi_\mu f_\mu$ where $f_\mu = f_\mu(\phi_\mu = 1)$ is the dimensionless specific Helmholtz free energy (per site) of pure component μ at unit volume fraction ϕ_μ.

V. Discussion

Our recent paper[10] presents a comparison of the lattice cluster theory predictions for a binary incompressible polymer–solvent system with Monte Carlo simulations for the same system. The comparison demonstrates that the cluster expansion provides a good approximation to the standard lattice model for this system. Additional theoretical computations[10] indicate a strong dependence of polymer properties on the structures of monomers and solvent molecules, which are both permitted to extend over several lattice sites. These results encourage us to generalize the LCT to multicomponent compressible polymer mixtures with arbitrary monomer structures (and solvent molecules). The multicomponent generalization is also required to consider polydispersity corrections and many interesting ternary mixtures. Compressibility, on the other hand, is known to profoundly affect excess thermodynamic properties, and its inclusion is a prerequisite to describing equations of state. However, the combination of many components, arbitrary monomer structures, and compressibility makes the original field theoretical lattice cluster computations for correction to Flory–Huggins theory extremely unwieldy.

The generalization of the LCT to compressible, multicomponent, and structured monomer–polymer systems is greatly facilitated by the new algebraic derivation of

Table II
Values of the First-Order Energy Diagrams Contributing to the Helmholtz Free Energy per Site through Order z^{-2} beyond the Leading FH Term for k-Component Polymer Mixture[a]

diagram of Figure 3	contribution from cumulant diagram	diagram of Figure 3	contribution from cumulant diagram
a	$C_0^{(\epsilon)} = \frac{z}{2}\sum_{\mu=1}^{k}\sum_{\eta=1}^{k}\epsilon_{\mu\eta}\phi_\mu\phi_\eta$	f_3	$C_{18}^{(\epsilon)} = \frac{1}{z}\sum_{\kappa=1}^{k}N(1,\kappa)N(2,\kappa)M_\kappa\phi_\kappa\epsilon_{\kappa\kappa}$
	$C'_0{}^{(\epsilon^2)} = \frac{z}{4}\sum_{\mu=1}^{k}\sum_{\eta=1}^{k}\epsilon_{\mu\eta}{}^2\phi_\mu\phi_\eta$	f_4	$C_{19}^{(\epsilon)} = \frac{4}{z}\sum_{\kappa=1}^{k}\sum_{\lambda=1}^{k}N(1,\kappa)N(2,\lambda)\phi_\kappa\phi_\lambda\sum_{\mu=1}^{k}\epsilon_{\kappa\mu}\phi_\mu - \frac{6}{z}\sum_{\kappa=1}^{k}\sum_{\lambda=1}^{k}N(1,\kappa)\times N(2,\lambda)\phi_\kappa\phi_\lambda\epsilon_{\kappa\kappa} - \frac{2}{z}\sum_{\kappa=1}^{k}N(1,\kappa)N(2,\kappa)M_\kappa\phi_\kappa\sum_{\mu=1}^{k}\epsilon_{\kappa\mu}\phi_\mu$
b_1	$C_1^{(\epsilon)} = \sum_{\kappa=1}^{k}N(1,\kappa)\phi_\kappa\sum_{\mu=1}^{k}\sum_{\eta=1}^{k}\epsilon_{\mu\eta}\phi_\mu\phi_\eta$		
	$C'_1{}^{(\epsilon^2)} = \frac{1}{2}\sum_{\kappa=1}^{k}N(1,\kappa)\phi_\kappa\sum_{\mu=1}^{k}\sum_{\eta=1}^{k}\epsilon_{\mu\eta}{}^2\phi_\mu\phi_\eta$	f_5	$C_{20}^{(\epsilon)} = -\frac{4}{z}\sum_{\kappa=1}^{k}\sum_{\lambda=1}^{k}N(1,\kappa)N(2,\lambda)\phi_\kappa\phi_\lambda\sum_{\mu=1}^{k}\epsilon_{\lambda\mu}\phi_\mu$
b_2	$C_2^{(\epsilon)} = -2\sum_{\kappa=1}^{k}N(1,\kappa)\phi_\kappa\sum_{\mu=1}^{k}\epsilon_{\kappa\mu}\phi_\mu$	f_6	$C_{21}^{(\epsilon)} = \frac{3}{2}C_{20}^{(\epsilon)}$
	$C'_2{}^{(\epsilon^2)} = -\sum_{\kappa=1}^{k}N(1,\kappa)\phi_\kappa\sum_{\mu=1}^{k}\epsilon_{\kappa\mu}{}^2\phi_\mu$	f_7	$C_{22}^{(\epsilon)} = -\frac{3}{2}C_{20}^{(\epsilon)} + \frac{1}{z}\sum_{\kappa=1}^{k}N(1,\kappa)N(2,\lambda)M_\kappa\phi_\kappa\sum_{\mu=1}^{k}\sum_{\eta=1}^{k}\epsilon_{\mu\eta}\phi_\mu\phi_\eta$
b_3	$C_3^{(\epsilon)} = \sum_{\kappa=1}^{k}N(1,\kappa)\phi_\kappa\epsilon_{\kappa\kappa}$	g_1	$C_{23}^{(\epsilon)} = -\frac{2}{z}\sum_{\kappa=1}^{k}\sum_{\lambda=1}^{k}[N(1,\kappa)]^2N(1,\lambda)M_\kappa\phi_\kappa\phi_\lambda\epsilon_{\kappa\kappa}$
	$C'_3{}^{(\epsilon^2)} = \frac{1}{2}\sum_{\kappa=1}^{k}N(1,\kappa)\phi_\kappa\epsilon_{\kappa\kappa}{}^2$	g_2	$C_{24}^{(\epsilon)} = -\frac{4}{z}\sum_{\kappa=1}^{k}\sum_{\lambda=1}^{k}\sum_{\mu=1}^{k}N(1,\kappa)N(1,\lambda)N(1,\mu)\phi_\kappa\phi_\lambda\phi_\mu\epsilon_{\kappa\lambda}$
c_1	$C_4^{(\epsilon)} = -\frac{2}{z}\sum_{\kappa=1}^{k}N(2,\kappa)\phi_\kappa\epsilon_{\kappa\kappa}$	g_3	$C_{25}^{(\epsilon)} = -2C_{24}^{(\epsilon)} + \frac{4}{z}\sum_{\kappa=1}^{k}\sum_{\lambda=1}^{k}[N(1,\kappa)]^2N(1,\lambda)M_\kappa\phi_\kappa\phi_\lambda\sum_{\mu=1}^{k}\epsilon_{\kappa\mu}\phi_\mu$
c_2	$C_5^{(\epsilon)} = \frac{2}{z}\sum_{\kappa=1}^{k}N(2,\kappa)\phi_\kappa\sum_{\mu=1}^{k}\epsilon_{\kappa\mu}\phi_\mu$	g_4	$C_{26}^{(\epsilon)} = \frac{4}{z}\sum_{\kappa=1}^{k}\sum_{\lambda=1}^{k}\sum_{\mu=1}^{k}N(1,\kappa)N(1,\lambda)N(1,\mu)\phi_\kappa\phi_\lambda\phi_\mu\sum_{\tau=1}^{k}\sum_{\eta=1}^{k}\epsilon_{\tau\eta}\phi_\tau\phi_\eta - \frac{8}{z}\sum_{\kappa=1}^{k}\sum_{\lambda=1}^{k}\sum_{\mu=1}^{k}N(1,\kappa)N(1,\lambda)N(1,\mu)\phi_\kappa\phi_\lambda\phi_\mu\sum_{\tau=1}^{k}\epsilon_{\kappa\tau}\phi_\tau - \frac{2}{z}\sum_{\kappa=1}^{k}\sum_{\lambda=1}^{k}[N(1,\kappa)]^2N(1,\lambda)M_\kappa\phi_\kappa\phi_\lambda\sum_{\mu=1}^{k}\sum_{\eta=1}^{k}\epsilon_{\mu\eta}\phi_\mu\phi_\eta$
c_3	$C_6^{(\epsilon)} = C_5^{(\epsilon)}$		
c_4	$C_7^{(\epsilon)} = -\frac{2}{z}\sum_{\kappa=1}^{k}N(2,\kappa)\phi_\kappa\sum_{\mu=1}^{k}\sum_{\eta=1}^{k}\epsilon_{\mu\eta}\phi_\mu\phi_\eta$		
d_1	$C_8^{(\epsilon)} = \frac{2}{z}\sum_{\kappa=1}^{k}\sum_{\lambda=1}^{k}N(1,\kappa)N(1,\lambda)\phi_\kappa\phi_\lambda\epsilon_{\kappa\kappa}$	h_1	$C_{27}^{(\epsilon)} = -\frac{1}{z}\sum_{\kappa=1}^{k}N(1,2;\kappa)\phi_\kappa\sum_{\mu=1}^{k}\sum_{\eta=1}^{k}\epsilon_{\mu\eta}\phi_\mu\phi_\eta$
d_2	$C_9^{(\epsilon)} = -\frac{8}{z}\sum_{\kappa=1}^{k}\sum_{\lambda=1}^{k}N(1,\kappa)N(1,\lambda)\phi_\kappa\phi_\lambda\sum_{\mu=1}^{k}\epsilon_{\kappa\mu}\phi_\mu$	h_2	$C_{28}^{(\epsilon)} = \frac{2}{z}\sum_{\kappa=1}^{k}N(1,2;\kappa)\phi_\kappa\sum_{\mu=1}^{k}\epsilon_{\kappa\mu}\phi_\mu$
d_3	$C_{10}^{(\epsilon)} = \frac{4}{z}\sum_{\kappa=1}^{k}\sum_{\lambda=1}^{k}N(1,\kappa)N(1,\lambda)\phi_\kappa\phi_\lambda\sum_{\mu=1}^{k}\sum_{\eta=1}^{k}\epsilon_{\mu\eta}\phi_\mu\phi_\eta$	h_3	$C_{29}^{(\epsilon)} = -\frac{1}{z}\sum_{\kappa=1}^{k}N(1,2;\kappa)\phi_\kappa\epsilon_{\kappa\kappa}$
d_4	$C_{11}^{(\epsilon)} = \frac{2}{z}\sum_{\kappa=1}^{k}\sum_{\lambda=1}^{k}N(1,\kappa)N(1,\lambda)\phi_\kappa\phi_\lambda\epsilon_{\kappa\lambda}$	i_1	$C_{30}^{(\epsilon)} = -\frac{3}{z}\sum_{\kappa=1}^{k}N(\perp,\kappa)\phi_\kappa\sum_{\mu=1}^{k}\sum_{\eta=1}^{k}\epsilon_{\mu\eta}\phi_\mu\phi_\eta$
e_1	$C_{12}^{(\epsilon)} = -\frac{2}{z}\sum_{\kappa=1}^{k}N(3,\kappa)\phi_\kappa\epsilon_{\kappa\kappa}$	i_2	$C_{31}^{(\epsilon)} = \frac{3}{z}\sum_{\kappa=1}^{k}N(\perp,\kappa)\phi_\kappa\sum_{\mu=1}^{k}\epsilon_{\kappa\mu}\phi_\mu$
e_2	$C_{13}^{(\epsilon)} = \frac{2}{z}\sum_{\kappa=1}^{k}N(3,\kappa)\phi_\kappa\sum_{\mu=1}^{k}\epsilon_{\kappa\mu}\phi_\mu$	i_3	$C_{32}^{(\epsilon)} = C_{31}^{(\epsilon)}$
e_3	$C_{14}^{(\epsilon)} = -\frac{1}{z}\sum_{\kappa=1}^{k}N(3,\kappa)\phi_\kappa\sum_{\mu=1}^{k}\sum_{\eta=1}^{k}\epsilon_{\mu\eta}\phi_\mu\phi_\eta$	i_4	$C_{33}^{(\epsilon)} = -\frac{3}{z}\sum_{\kappa=1}^{k}N(\perp,\kappa)\phi_\kappa\epsilon_{\kappa\kappa}$
e_4	$C_{15}^{(\epsilon)} = -\frac{1}{2}C_{12}^{(\epsilon)}$	j_1	$C_{34}^{(\epsilon)} = \frac{4}{z}\sum_{\kappa=1}^{k}\sum_{\lambda=1}^{k}N(1,\kappa)N(1,1;\lambda)\phi_\kappa\phi_\lambda\sum_{\mu=1}^{k}\sum_{\eta=1}^{k}\epsilon_{\mu\eta}\phi_\mu\phi_\eta$
f_1	$C_{16}^{(\epsilon)} = \frac{2}{z}\sum_{\kappa=1}^{k}\sum_{\lambda=1}^{k}N(1,\kappa)N(2,\lambda)\phi_\kappa\phi_\lambda\epsilon_{\kappa\lambda}$	j_2	$C_{35}^{(\epsilon)} = -\frac{8}{z}\sum_{\kappa=1}^{k}\sum_{\lambda=1}^{k}N(1,\kappa)N(1,1;\lambda)\phi_\kappa\phi_\lambda\sum_{\mu=1}^{k}\epsilon_{\lambda\mu}\phi_\mu$
f_2	$C_{17}^{(\epsilon)} = \frac{4}{z}\sum_{\kappa=1}^{k}\sum_{\lambda=1}^{k}N(1,\kappa)N(2,\lambda)\phi_\kappa\phi_\lambda\epsilon_{\lambda\lambda}$	j_3	$C_{36}^{(\epsilon)} = \frac{4}{z}\sum_{\kappa=1}^{k}\sum_{\lambda=1}^{k}N(1,\kappa)N(1,1;\lambda)\phi_\kappa\phi_\lambda\epsilon_{\lambda\lambda}$

[a] $N(i,\alpha) \equiv N_i^{(\alpha)}/M_\alpha$, $\alpha = 1, 2, \ldots, k$; $N(i,j;\alpha) \equiv N_{ij}{}^{(\alpha)}/M_\alpha$, $\alpha = 1, 2, \ldots, k$; $\phi_\alpha = n_\alpha M_\alpha/N_l$, $\alpha = 1, 2, \ldots, k$; $\sum_{\alpha=1}^{k}\phi_\alpha + \phi_v = 1$ and all interaction energies ϵ are in units of k_BT.

Table III. Values of the Second-Order Energy Diagrams Contributing to the Helmholtz Free Energy per Site through Order z^{-1} beyond the Leading EMF Term for k-Component Polymer Mixture[a]

diagram of Figure 4	contribution from cumulant diagram
a_1	$C_1^{(\epsilon^2)} = -\frac{z}{2}\sum_{\mu=1}^{k}\sum_{\eta=1}^{k}\sum_{\omega=1}^{k}\epsilon_{\mu\eta}\epsilon_{\eta\omega}\phi_\mu\phi_\eta\phi_\omega$
a_2	$C_2^{(\epsilon^2)} = \frac{z}{4}\sum_{\mu=1}^{k}\sum_{\eta=1}^{k}\sum_{\omega=1}^{k}\sum_{\tau=1}^{k}\epsilon_{\mu\eta}\epsilon_{\omega\tau}\phi_\mu\phi_\eta\phi_\omega\phi_\tau$
b_1	$C_3^{(\epsilon^2)} = -2\sum_{\kappa=1}^{k}N(1,\kappa)\phi_\kappa\epsilon_{\kappa\kappa}\sum_{\mu=1}^{k}\epsilon_{\kappa\mu}\phi_\mu$
b_2	$C_4^{(\epsilon^2)} = 2\sum_{\kappa=1}^{k}N(1,\kappa)\phi_\kappa\sum_{\mu=1}^{k}\sum_{\eta=1}^{k}\epsilon_{\kappa\mu}\epsilon_{\mu\eta}\phi_\mu\phi_\eta$
b_3	$C_5^{(\epsilon^2)} = 2\sum_{\kappa=1}^{k}N(1,\kappa)\phi_\kappa\sum_{\mu=1}^{k}\sum_{\eta=1}^{k}\epsilon_{\kappa\mu}\epsilon_{\kappa\eta}\phi_\mu\phi_\eta$
b_4	$C_6^{(\epsilon^2)} = -2\sum_{\kappa=1}^{k}N(1,\kappa)\phi_\kappa\sum_{\mu=1}^{k}\sum_{\eta=1}^{k}\sum_{\omega=1}^{k}\epsilon_{\mu\eta}\epsilon_{\eta\omega}\phi_\mu\phi_\eta\phi_\omega$
b_5	$C_7^{(\epsilon^2)} = \sum_{\kappa=1}^{k}N(1,\kappa)\phi_\kappa\epsilon_{\kappa\kappa}\sum_{\mu=1}^{k}\sum_{\eta=1}^{k}\epsilon_{\mu\eta}\phi_\mu\phi_\eta$
b_6	$C_8^{(\epsilon^2)} = -4\sum_{\kappa=1}^{k}N(1,\kappa)\phi_\kappa\sum_{\mu=1}^{k}\sum_{\eta=1}^{k}\sum_{\omega=1}^{k}\epsilon_{\kappa\mu}\epsilon_{\eta\omega}\phi_\mu\phi_\eta\phi_\omega$
b_7	$C_9^{(\epsilon^2)} = \frac{1}{2}C_5^{(\epsilon^2)}$
b_8	$C_{10}^{(\epsilon^2)} = 2\sum_{\kappa=1}^{k}N(1,\kappa)\phi_\kappa\sum_{\mu=1}^{k}\sum_{\eta=1}^{k}\sum_{\omega=1}^{k}\sum_{\tau=1}^{k}\epsilon_{\mu\eta}\epsilon_{\omega\tau}\phi_\mu\phi_\eta\phi_\omega\phi_\tau$
c_1	$C_{11}^{(\epsilon^2)} = \frac{3}{2}\sum_{\kappa=1}^{k}N(2,\kappa)\phi_\kappa\sum_{\mu=1}^{k}\sum_{\eta=1}^{k}\epsilon_{\kappa\mu}\epsilon_{\kappa\eta}\phi_\mu\phi_\eta$
c_2	$C_{12}^{(\epsilon^2)} = -2\sum_{\kappa=1}^{k}N(2,\kappa)\phi_\kappa\epsilon_{\kappa\kappa}\sum_{\mu=1}^{k}\epsilon_{\kappa\mu}\phi_\mu$
c_3	$C_{13}^{(\epsilon^2)} = \sum_{\kappa=1}^{k}N(2,\kappa)\phi_\kappa{\epsilon_{\kappa\kappa}}^2$
c_4	$C_{14}^{(\epsilon^2)} = \sum_{\kappa=1}^{k}N(2,\kappa)\phi_\kappa\sum_{\mu=1}^{k}{\epsilon_{\kappa\mu}}^2\phi_\mu$
c_5	$C_{15}^{(\epsilon^2)} = \sum_{\kappa=1}^{k}N(2,\kappa)\phi_\kappa\sum_{\mu=1}^{k}\sum_{\eta=1}^{k}\epsilon_{\kappa\mu}\epsilon_{\mu\eta}\phi_\mu\phi_\eta$
c_6	$C_{16}^{(\epsilon^2)} = \frac{2}{3}C_{11}^{(\epsilon^2)}$
c_7	$C_{17}^{(\epsilon^2)} = -3C_{15}^{(\epsilon^2)} - C_{11}^{(\epsilon^2)} + \sum_{\kappa=1}^{k}N(2,\kappa)\phi_\kappa\sum_{\mu=1}^{k}\sum_{\eta=1}^{k}\sum_{\omega=1}^{k}\epsilon_{\mu\eta}\epsilon_{\eta\omega}\phi_\mu\phi_\eta\phi_\omega$
c_8	$C_{18}^{(\epsilon^2)} = 2\sum_{\kappa=1}^{k}N(2,\kappa)\phi_\kappa\epsilon_{\kappa\kappa}\sum_{\mu=1}^{k}\sum_{\eta=1}^{k}\epsilon_{\mu\eta}\phi_\mu\phi_\eta$
c_9	$C_{19}^{(\epsilon^2)} = \frac{4}{3}C_{11}^{(\epsilon^2)}$
c_{10}	$C_{20}^{(\epsilon^2)} = C_{12}^{(\epsilon^2)}$
c_{11}	$C_{21}^{(\epsilon^2)} = -3\sum_{\kappa=1}^{k}N(2,\kappa)\phi_\kappa\sum_{\mu=1}^{k}\sum_{\eta=1}^{k}\sum_{\omega=1}^{k}\epsilon_{\kappa\mu}\epsilon_{\eta\omega}\phi_\mu\phi_\eta\phi_\omega$
c_{12}	$C_{22}^{(\epsilon^2)} = \frac{2}{3}C_{21}^{(\epsilon^2)}$
c_{13}	$C_{23}^{(\epsilon^2)} = -C_{21}^{(\epsilon^2)}$
d_1	$C_{24}^{(\epsilon^2)} = -4\sum_{\kappa=1}^{k}\sum_{\lambda=1}^{k}N(1,\kappa)N(1,\lambda)\phi_\kappa\phi_\lambda\epsilon_{\kappa\lambda}\epsilon_{\kappa\kappa}$
d_2	$C_{25}^{(\epsilon^2)} = 4\sum_{\kappa=1}^{k}\sum_{\lambda=1}^{k}N(1,\kappa)N(1,\lambda)\phi_\kappa\phi_\lambda\epsilon_{\kappa\lambda}\sum_{\mu=1}^{k}\epsilon_{\kappa\mu}\phi_\mu$
d_3	$C_{26}^{(\epsilon^2)} = 4\sum_{\kappa=1}^{k}\sum_{\lambda=1}^{k}N(1,\kappa)N(1,\lambda)\phi_\kappa\phi_\lambda\epsilon_{\kappa\kappa}\sum_{\mu=1}^{k}\epsilon_{\kappa\mu}\phi_\mu$
d_4	$C_{27}^{(\epsilon^2)} = -6\sum_{\kappa=1}^{k}\sum_{\lambda=1}^{k}N(1,\kappa)N(1,\lambda)\phi_\kappa\phi_\lambda\sum_{\mu=1}^{k}\sum_{\eta=1}^{k}\epsilon_{\kappa\mu}\epsilon_{\kappa\eta}\phi_\mu\phi_\eta$
d_5	$C_{28}^{(\epsilon^2)} = -4\sum_{\kappa=1}^{k}\sum_{\lambda=1}^{k}N(1,\kappa)N(1,\lambda)\phi_\kappa\phi_\lambda\sum_{\mu=1}^{k}\sum_{\eta=1}^{k}\epsilon_{\kappa\mu}\epsilon_{\mu\eta}\phi_\mu\phi_\eta$
d_6	$C_{29}^{(\epsilon^2)} = -\frac{1}{3}C_{27}^{(\epsilon^2)} - C_{28}^{(\epsilon^2)}$
d_7	$C_{30}^{(\epsilon^2)} = -2\sum_{\kappa=1}^{k}\sum_{\lambda=1}^{k}N(1,\kappa)N(1,\lambda)\phi_\kappa\phi_\lambda\epsilon_{\kappa\lambda}\sum_{\mu=1}^{k}\sum_{\eta=1}^{k}\epsilon_{\mu\eta}\phi_\mu\phi_\eta$
d_8	$C_{31}^{(\epsilon^2)} = \sum_{\kappa=1}^{k}\sum_{\lambda=1}^{k}N(1,\kappa)N(1,\lambda){\epsilon_{\kappa\lambda}}^2\phi_\kappa\phi_\lambda$
d_9	$C_{32}^{(\epsilon^2)} = -C_{24}^{(\epsilon^2)} + 2\sum_{\kappa=1}^{k}[N(1,\kappa)]^2M_\kappa\phi_\kappa\sum_{\mu=1}^{k}\epsilon_{\kappa\mu}\phi_\mu$
d_{10}	$C_{33}^{(\epsilon^2)} = -2C_{25}^{(\epsilon^2)} + 2\sum_{\kappa=1}^{k}\sum_{\lambda=1}^{k}N(1,\kappa)N(1,\lambda)\phi_\kappa\phi_\lambda \times [2\sum_{\mu=1}^{k}\sum_{\eta=1}^{k}\epsilon_{\kappa\mu}\epsilon_{\lambda\eta}\phi_\mu\phi_\eta - \sum_{\mu=1}^{k}\epsilon_{\kappa\mu}\epsilon_{\lambda\mu}\phi_\mu] - 2\sum_{\kappa=1}^{k}[N(1,\kappa)]^2M_\kappa\phi_\kappa\sum_{\mu=1}^{k}\sum_{\eta=1}^{k}\epsilon_{\kappa\mu}\epsilon_{\kappa\eta}\phi_\mu\phi_\eta$
d_{11}	$C_{34}^{(\epsilon^2)} = -\frac{1}{2}\sum_{\kappa=1}^{k}[N(1,\kappa)]^2M_\kappa\phi_\kappa{\epsilon_{\kappa\kappa}}^2$
d_{12}	$C_{35}^{(\epsilon^2)} = \frac{1}{3}C_{27}^{(\epsilon^2)}$
d_{13}	$C_{36}^{(\epsilon^2)} = -C_{26}^{(\epsilon^2)} - \sum_{\kappa=1}^{k}[N(1,\kappa)]^2M_\kappa\phi_\kappa\epsilon_{\kappa\kappa}\sum_{\mu=1}^{k}\sum_{\eta=1}^{k}\epsilon_{\mu\eta}\phi_\mu\phi_\eta$
d_{14}	$C_{37}^{(\epsilon^2)} = -\frac{4}{3}C_{27}^{(\epsilon^2)} - C_{28}^{(\epsilon^2)} - 2C_{30}^{(\epsilon^2)} + 2\sum_{\kappa=1}^{k}[N(1,\kappa)]^2M_\kappa\phi_\kappa\sum_{\mu=1}^{k}\sum_{\eta=1}^{k}\sum_{\omega=1}^{k}\epsilon_{\kappa\mu}\epsilon_{\eta\omega}\phi_\mu\phi_\eta\phi_\omega$
d_{15}	$C_{38}^{(\epsilon^2)} = \sum_{\kappa=1}^{k}\sum_{\lambda=1}^{k}N(1,\kappa)N(1,\lambda)\phi_\kappa\phi_\lambda \times \{3\sum_{\mu=1}^{k}\sum_{\eta=1}^{k}\sum_{\omega=1}^{k}\sum_{\tau=1}^{k}\epsilon_{\mu\eta}\epsilon_{\omega\tau}\phi_\mu\phi_\eta\phi_\omega\phi_\tau - 2\sum_{\mu=1}^{k}\sum_{\eta=1}^{k}\sum_{\omega=1}^{k}[\epsilon_{\mu\eta}\epsilon_{\eta\omega} + 4\epsilon_{\kappa\mu}\epsilon_{\eta\omega}]\} - \frac{1}{2}\sum_{\kappa=1}^{k}[N(1,\kappa)]^2M_\kappa\phi_\kappa \times \sum_{\mu=1}^{k}\sum_{\eta=1}^{k}\sum_{\omega=1}^{k}\sum_{\tau=1}^{k}\epsilon_{\mu\eta}\epsilon_{\omega\tau}\phi_\mu\phi_\eta\phi_\omega\phi_\tau$
e_1	$C_{39}^{(\epsilon^2)} = \sum_{\kappa=1}^{k}N(1,1;\kappa)\phi_\kappa\sum_{\mu=1}^{k}\sum_{\eta=1}^{k}\sum_{\omega=1}^{k}\sum_{\tau=1}^{k}\epsilon_{\mu\eta}\epsilon_{\omega\tau}\phi_\mu\phi_\eta\phi_\omega\phi_\tau$
e_2	$C_{40}^{(\epsilon^2)} = -4\sum_{\kappa=1}^{k}N(1,1;\kappa)\phi_\kappa\sum_{\mu=1}^{k}\sum_{\eta=1}^{k}\sum_{\omega=1}^{k}\epsilon_{\kappa\mu}\epsilon_{\eta\omega}\phi_\mu\phi_\eta\phi_\omega$
e_3	$C_{41}^{(\epsilon^2)} = 2\sum_{\kappa=1}^{k}N(1,1;\kappa)\phi_\kappa\epsilon_{\kappa\kappa}\sum_{\mu=1}^{k}\sum_{\eta=1}^{k}\epsilon_{\mu\eta}\phi_\mu\phi_\eta$
e_4	$C_{42}^{(\epsilon^2)} = \sum_{\kappa=1}^{k}N(1,1;\kappa){\epsilon_{\kappa\kappa}}^2\phi_\kappa$
e_5	$C_{43}^{(\epsilon^2)} = 4\sum_{\kappa=1}^{k}N(1,1;\kappa)\phi_\kappa\sum_{\mu=1}^{k}\sum_{\eta=1}^{k}\epsilon_{\kappa\mu}\epsilon_{\kappa\eta}\phi_\mu\phi_\eta$
e_6	$C_{44}^{(\epsilon^2)} = -4\sum_{\kappa=1}^{k}N(1,1;\kappa)\phi_\kappa\epsilon_{\kappa\kappa}\sum_{\mu=1}^{k}\epsilon_{\kappa\mu}\phi_\mu$

[a] $N(i,\alpha) \equiv N_i^{(\alpha)}/M_\alpha$, $\alpha = 1, 2, ..., k$; $N(i,j;\alpha) \equiv N_{i,j}^{(\alpha)}/M_\alpha$, $\alpha = 1, 2, ..., k$; $\phi_\alpha = n_\alpha M\alpha/N_l$, $\alpha = 1, 2, ..., k$; $\sum_{\alpha=1}^{k}\phi_\alpha + \phi_v = 1$ and all interaction ϵ are in units k_BT.

the LCT in which the counting rules for energy diagrams and the theorem on the exact cancellation of the $\mathbf{q} = 0$ energy terms (see Appendix A) follow in a natural manner from the Mayer cluster form of the partition function 3.3. The original field theory formulation of the LCT does not make these features obvious or tractable to derive. The present paper provides the derivation of these new results, some of which have already been used in our previous article on incompressible binary polymer systems.[10] The generalized LCT is therefore developed here as a powerful tool for studing thermodynamic properties of many different multicomponent polymer mixtures. This new formulation of the LCT currently precludes considering situations with strong, polar interactions as expansions are made in powers of the ratio of interaction energies to the thermal energy k_BT. Nevertheless, a wide range of interesting polymer systems falls within the confines of these constraints, and our goal is in describing some of their rich and varied behavior.

The lattice cluster theory introduces the spatially short range bonding-induced correlations that are entirely ignored in classic Flory–Huggins theory. These correlations between bonds on the same and different polymers are represented in the terms of Mayer-like diagrams involving the correlating bonds and their van der Waals interactions. Corrections to the mean field athermal limit entropy are presented in Table I, and they depend on the number k of components in the system, their molecular weights, and a set of counting indexes $N_i^{(\mu)}$ that characterize the monomer molecular structures and overall chain architectures. This athermal noncombinatorial entropy is produced by the LCT as a series in z^{-1}, where the lattice coordination number z equals the number of nearest neighbors to a lattice site. Coefficients in this expansion are simple polynomials in compositions and in the monomer structure dependent counting indexes $N_i^{(\mu)}$, thereby providing an algebraic tractable, albeit lengthy, formulation of the statistical thermodynamics of multicomponent polymer systems. This algebraic simplicity contrasts with quasiclassical treatments, which contain an increasing number of algebraically complicated nonlinear constraints as the number of components grows. In addition, the LCT is found in our previous paper[10] to be of greater accuracy in reproducing Monte Carlo simulations for the polymer–solvent system.

The energetic corrections to Flory–Huggins theory are presented in Tables II and III as a double series in z^{-1} and the $k(k+1)/2$ nearest-neighbor attractive van der Waals energies $\epsilon_{\mu\lambda}$ (in units of k_BT). The coefficients again are simple polynomials in volume fractions and the counting indexes $N_i^{(\mu)}$, and they reflect the fact that contact probabilities are both functions of composition and molecular structure. The latter features are completely neglected in Flory–Huggins theory, are only partially included for linear chains in Guggenheim theories,[12] and are modeled by phenomenological surface fraction parameters in equation of state theories. Thus, the LCT Helmholtz free energy of mixing ΔF^{mix} and all thermodynamic quantities derived from ΔF^{mix} have corrections to FH theory that are polynomials in composition and that are valid for all energies $\epsilon_{\mu\lambda}/k_BT < 1$, temperatures T, site occupancy indexes M_i (proportional to the molecular weights), compositions, numbers of components, and monomer molecular weights. This analytical tractability and the enormous generality of the theory strongly offsets limitations inherent to any lattice model in faithfully representing polymer properties. Note that F or ΔF^{mix} in Tables I and II cannot be written in a pairwise additive form as is often assumed for multicomponent systems. Lack of that structure arises because of the existence of correlations between portions of more than two spatially nearby chains. These contributions are represented by diagrams in Figures 2 and 3 with more than two chains. The nonadditivity of the energy is further illustrated in the tables of the accompanying paper, which specializes to binary compressible blends.

The individual polymer volume fractions ϕ_μ satisfy the relation $\sum_{\mu=1}^{k}\phi_\mu = 1 - \phi_v$, where ϕ_v is the volume fraction for excess free volume. The excess free volume is given physical interpretation through the relation $\phi_v V = V - V^*$, with V^* the analog of the closed-packed volume in continuum model theories. The existence of free volume is necessary in order to describe the compressibility of the system, especially to describe what has been termed "equation of state effects" in the literature[19] and what corresponds to the thermodynamic consequences of volume changes upon mixing that may arise in compressible systems. An alternative representation involves use of the equation of state to eliminate ϕ_v in favor of the pressure P and the Gibbs free energy G. The latter is the representation employed in the numerical illustrations given in the following and subsequent papers.

The implications of the LCT are numerous. In addition to enabling the calculations of the small-angle neutron scattering Flory effective parameter χ_{eff} and other thermodynamic quantities, the LCT can produce the distribution functions $g_{\mu\lambda}(a)$ for the any $\mu\lambda$ nearest-neighbor segment pairs. The derivative $\partial[F/(N_lk_BT)]/\partial\epsilon_{\mu\lambda}$ yields the nearest-neighbor value of $g_{\mu\lambda}(a) = h_{\mu\lambda}(a) - 1$, where a is the lattice constant for cubic lattices. The presence of higher powers in $\epsilon_{\mu\lambda}/k_BT$ in the LCT leads to a temperature dependence of contact probabilities, while $g_{\mu\lambda}(a)$ depends on counting indexes $N_i^{(\mu)}$. Hence, monomer (and solvent molecule) structures affect contact probabilities. Including next-nearest-neighbor interactions, etc., into the Helmholtz free energy F provides the possibility for calculating the more distant portions of the distribution functions $g_{\mu\lambda}(r)$.

A comparison between the generalized compressible multicomponent polymer mixture LCT and other theories of the liquid state produces other interesting conclusions. For example, the most advanced of the van der Waals fluid theories,[20] the three-fluid model, does not describe higher order correlation terms which the LCT incorporates. The Gibbs free energy of the van der Waals three-fluid model mixtures can be written[20] as

$$G = Nk_BT\sum_{\alpha} x_\alpha \ln x_\alpha + \sum_{\alpha}\sum_{\beta} x_\alpha x_\beta G_{\alpha\beta} \qquad (5.1)$$

where $G_{\alpha\beta}$ does not depend on the mole fractions x_i, $i = \alpha, \beta$, which correspond to the volume fractions Φ_i in our notation. The lattice cluster theory Helmholtz free energy F reduces to the pairwise additive form of (5.1) only upon neglect of the corrections to the mean field FH approximations that are represented by the "entropy" diagrams e, k, m, and n in Figure 2 and by the energy diagrams b_1, c_4, d_2, d_3, f_4–h_1, i_1, j_1, j_2 and a_1, a_2, b_2–c_1, c_5–c_9, c_{11}–c_{13}, d_2–d_7, d_9, d_{10}, d_{12}–e_3, e_5 of Figures 3 and 4. (Higher order LCT corrections yield additional nonadditive terms.) Extra nonadditivity effects appear in the LCT upon transformation from F to G. In this process the volume fraction ϕ_v is replaced by a nonlinear function $\phi_v(\Phi_1)$ as determined from the equation of state. Additional violations of the pairwise additivity for $G = F + PV$ emerge from the factor of the pressure P, which by the equation of state is a non-

linear function of ϕ_v. A comparison of the LCT predictions with RISM integral equation theory computations of Schweizer and Curro[21] is provided through the numerical illustrations in the following paper.

The LCT is amenable to many systematic improvements by introducing a more adequate description of the entropy associated with the distribution of free volume, a more accurate representation of interaction energies, and a treatment of chain stiffness. First, it is possible to describe[22] semiflexible polymer architectures, but this has only been accomplished so far in the lowest order. Second, allowing chemically different groups of the same monomer to interact with different energies would make the model more realistic, but the algebraic expressions rapidly become more lengthy. The FH treatment of the free volume entropy adversely affects predictions in the high-pressure range and persists similarly in the LCT. This deficiency of the lattice model may be rectified by replacing the lattice free volume entropic contribution $N_l k_B T \phi_v \ln \phi_v$ by forms developed in the Flory equation of state theory[19] and in generalizations of Flory's theory that Dickman and Hall[23] and Honnell and Hall[24] have devised to rectify the classic FH theory treatment of free volume entropy. Another possible modification of the lattice model involves the calculation of the interaction energies from, for example, Lennard-Jones potentials[25] as a function of the lattice constant a. The free energy F is then minimized with respect to a.

Our present LCT theory provides a single very convenient analytical formula for the Helmholtz free energy F which is valid for all compositions Φ_i, $i = 1, ..., k-1$, molecular weights, monomer and solvent structures, number k of components, attractive van der Waals nearest-neighbor interaction energies $\epsilon_{\mu\lambda}$, $\mu, \lambda = 1, ..., k$, temperatures T, and pressures P. Examples illustrating typical predictions of the LCT are described in the following paper, while a detailed comparison of the LCT predictions with experimental data for the PS/PVME blends as well as a discussion of the role of monomer molecular structure and compressibility on the small-angle neutron scattering and thermodynamic properties of binary polymer blends will be presented in paper 3. There are clearly more possible interesting applications of the LCT than we can possibly treat in a few papers.

Acknowledgment. This research is supported, in part, by NSF Grant DMR 89-19941. We are grateful to Shawn Huston and Adolfo Nemirovsky for comments on the manuscript.

Appendix A: Proof of Theorem Concerning q = 0 Energetic Contributions

In the diagrammatic representation 3.9 of the Helmholtz free energy, the entropy and energy diagrams arise due to the correlations between monomer positions that are produced by the excluded volume constraints and nearest-neighbor van der Waals interactions, respectively. Thus, the entropy diagrams delineate various combinations of correlating bonds in the system, while the energy diagrams may have correlating bonds in addition to interaction lines. According to the counting rules described in sections II and III, the evaluation of entropy and energy diagrams is carried out in discrete Fourier space. Consequently, the procedure involves the summation over all $\{\mathbf{q}\}$ in the first Brillouin zone. The $\{\mathbf{q} = 0\}$ portion from all bonds produces the FH mean field combinatorial entropy (see eqs 2.6–2.8), while summation over the remaining nonzero values $\{\mathbf{q} \neq 0\}$ yields entropic corrections to FH arising from the spatial correlations between chain segments. The energetic corrections to FH come from interactions of the monomer pairs represented in a diagram by interaction lines. The main difference between these interaction lines and correlating bonds lies in the appearance of the additional $\mathbf{q} = 0$ term for the former.

When these $\mathbf{q} = 0$ contributions are added together for all energy diagrams, the results cancel exactly apart from the $\mathbf{q} = 0$ term of the leading diagram a of Figure 3, which just recovers the FH interaction energy. To prove this theorem, we begin separating the $\mathbf{q} = 0$ and $\mathbf{q} \neq 0$ contributions in the Boltzmann factor (3.1) by writing

$$\exp\Big[\sum_{\mu=1}^{k}\sum_{\lambda\le\mu}\sum_{\substack{i\in S_\mu\\ j\in S_\lambda}}{}'\epsilon_{\mu\lambda}^{ij}\Big] = \prod_{\mu=1}^{k}\prod_{\lambda\le\mu}\prod_{\substack{i\in S_\mu\\ j\in S_\lambda}}{}'\Big[1 + \sum_{\beta=1}^{z}\delta(i,j+\beta)\, f_{\mu\lambda}\Big] \tag{A.1}$$

Replacing each Kronecker δ in (A.1) by its lattice Fourier transform (2.3) and using eq 2.3a we obtain

$$\exp\Big[\sum_{\mu=1}^{k}\sum_{\lambda\le\mu}\sum_{\substack{i\in S_\mu\\ j\in S_\lambda}}{}'\epsilon_{\mu\lambda}^{ij}\Big] = \prod_{\mu=1}^{k}\prod_{\lambda\le\mu}\prod_{\substack{i\in S_\mu\\ j\in S_\lambda}}{}'\Big[1 + \frac{z}{N_l}f_{\mu\lambda} + \frac{f_{\mu\lambda}}{N_l}\times \sum_{\mathbf{q}\neq 0} f(\mathbf{q})\exp[i\mathbf{q}\cdot(\mathbf{r}_i - \mathbf{r}_j)]\Big] \tag{A.2}$$

Equivalently (A.2) may be rewritten as

$$\exp\Big[\sum_{\mu=1}^{k}\sum_{\lambda\le\mu}\sum_{\substack{i\in S_\mu\\ j\in S_\lambda}}{}'\epsilon_{\mu\lambda}^{ij}\Big] = \prod_{\mu=1}^{k}\prod_{\lambda\le\mu}\prod_{\substack{i\in S_\mu\\ j\in S_\lambda}}{}'\Big\{\Big[1 + f_{\mu\lambda}\frac{z}{N_l}\Big]\times \Big[1 + \frac{f_{\mu\lambda}}{N_l\Big(1 + f_{\mu\lambda}\frac{z}{N_l}\Big)}\sum_{\mathbf{q}\neq 0} f(\mathbf{q})\exp[i\mathbf{q}\cdot(\mathbf{r}_i - \mathbf{r}_j)]\Big]\Big\} \tag{A.3}$$

It is convenient to replace the products over μ and $\lambda \le \mu$ in (A.3) by the products over μ and over (μ and $\lambda < \mu$)

$$\exp\Big[\sum_{\mu=1}^{k}\sum_{\lambda\le\mu}\sum_{\substack{i\in S_\mu\\ j\in S_\lambda}}{}'\epsilon_{\mu\lambda}^{ij}\Big] = \Big\{\prod_{\mu=1}^{k}\prod_{\substack{i,j\in S_\mu\\ i>j}}\Big[1 + f_{\mu\mu}\frac{z}{N_l}\Big]\times \Big[1 + \frac{f_{\mu\mu}}{N_l\Big(1 + f_{\mu\mu}\frac{z}{N_l}\Big)}\sum_{\mathbf{q}\neq 0} f(\mathbf{q})\exp[i\mathbf{q}\cdot(\mathbf{r}_i - \mathbf{r}_j)]\Big]\Big\}\times \Big\{\prod_{\mu=1}^{k}\prod_{\lambda<\mu}\prod_{\substack{i\in S_\mu\\ j\in S_\lambda}}\Big[1 + f_{\mu\lambda}\frac{z}{N_l}\Big]\times \Big[1 + \frac{f_{\mu\lambda}}{N_l\Big(1 + f_{\mu\lambda}\frac{z}{N_l}\Big)}\sum_{\mathbf{q}\neq 0} f(\mathbf{q})\exp[i\mathbf{q}\cdot(\mathbf{r}_i - \mathbf{r}_j)]\Big]\Big\} \tag{A.4}$$

The factors $1 + f_{\mu\mu}z/N_l$ and $1 + f_{\mu\lambda}z/N_l$ in (A.4) do not depend on i and j. Consequently, their product over all

i–j pairs yields

$$\exp[\sum_{\mu=1}^{k}\sum_{\lambda\le\mu}\sum_{\substack{i\in S_\mu\\ j\in S_\lambda}}{}' \epsilon_{\mu\lambda}^{ij}] = \left\{\prod_{\mu=1}^{k}\left[1+f_{\mu\mu}\frac{z}{N_l}\right]^{n_\mu M_\mu(n_\mu M_\mu-1)/2!}\prod_{\substack{i,j\in S_\mu\\ i>j}}\left[1+\frac{f_{\mu\mu}}{N_l\left(1+f_{\mu\mu}\frac{z}{N_l}\right)}\times\sum_{\mathbf{q}\neq 0} f(\mathbf{q})\exp[i\mathbf{q}\cdot(\mathbf{r}_i-\mathbf{r}_j)]\right]\right\}\left\{\prod_{\mu=1}^{k}\prod_{\lambda>\mu}\left[1+f_{\mu\lambda}\frac{z}{N_l}\right]^{n_\mu M_\mu n_\lambda M_\lambda}\times\prod_{\substack{i\in S_\mu\\ j\in S_\lambda}}\left[1+\frac{f_{\mu\lambda}}{N_l\left(1+f_{\mu\lambda}\frac{z}{N_l}\right)}\times\sum_{\mathbf{q}\neq 0}(\mathbf{q})\exp[i\mathbf{q}\cdot(\mathbf{r}_i-\mathbf{r}_j)]\right]\right\} \quad (A.5)$$

Equation A.5 contains $X^{\mu}_{\alpha,m}$ of (2.6b) with the coefficients quoted in (3.7) as arising from the removal of $\mathbf{q} = 0$ terms.

The $\mathbf{q} = 0$ energy contributions $E_{\mathbf{q}=0}$ to the Helmholtz free energy $F(\{n_\mu\},\{N_\mu\})$ emerge directly from (A.5) by taking the logarithm of the right-hand side and expanding in a Taylor series. The $X^{\mu}_{\alpha,m}$-independent factors from (A.5) yield

$$\frac{E_{\mathbf{q}=0}}{k_BT} = -\sum_{\mu=1}^{k}\frac{n_\mu M_\mu(n_\mu M_\mu-1)}{2}\left[\frac{z}{N_l}f_{\mu\mu}-\frac{1}{2}\left(\frac{z}{N_l}f_{\mu\mu}\right)^2+\dots\right]- \sum_{\mu=1}^{k}\sum_{\lambda<\mu} n_\mu M_\mu n_\lambda M_\lambda\left[\frac{z}{N_l}f_{\mu\lambda}-\frac{1}{2}\left(\frac{z}{N_l}f_{\mu\lambda}\right)^2+\dots\right] \quad (A.6)$$

Retaining in (A.6) only terms proportional to N_l, since lower order terms in N_l vanish in the thermodynamic limit, leads to the simpler formula

$$\frac{E_{\mathbf{q}=0}}{k_BT} = -N_l\frac{z}{2}\sum_{\mu=1}^{k}\phi_\mu{}^2 f_{\mu\mu} - N_l z\sum_{\mu=1}^{k}\sum_{\lambda<\mu}\phi_\mu\phi_\lambda f_{\mu\lambda} = -N_l\frac{z}{2}\sum_{\mu=1}^{k}\sum_{\lambda=1}^{k}\phi_\mu\phi_\lambda f_{\mu\lambda} \quad (A.7)$$

Expanding the Mayer f function $f_{\mu\lambda}$ in a power series of $\epsilon_{\mu\lambda}$, in (A.7) recovers the FH interaction energy (denoted as $C_0^{(\epsilon)}$ in Table I) along with some EMF uncorrelated contributions of higher orders.

Appendix B: Athermal Entropy Diagrams for Multicomponent System

An entropy diagram depicts a toplogical set of B polymer bonds chosen from all bonds in the system and belonging to various polymer species $\mu = 1, 2, \dots, k$. Thus, specifying the number of bonds alone does not fully describe the entropy diagram, except the diagram with $B = 1$. A complete specification must include information on whether the correlating bonds belong to one chain or to many. For the former case, a designation of the relative bond positions is also required since sequential and nonsequential bonds contribute to the correlation terms $X^{\mu'}_{\alpha',m'}$, $X^{\mu'}_{\alpha',m'}X^{\mu''}_{\alpha'',m''}$, ... of (2.10) in different ways. Bonds selected from different chains are represented diagrammatically by disconnected lines to distinguish them from sequential bonds of one chain, while nonsequential bonds of the same chain are connected in a diagram by the wiggly lines (see diagrams j, l, and n of Figure 2).

The evaluation of the athermal limit entropy diagrams proceeds along the rules summarized in sections II and IV, and here we illustrate the counting process with reference to a particular diagram of order z^{-2}. Consider, for simplicity, a binary blend and evaluate diagram k of Figure 2 with $B = 4$ correlating bonds, two of which are sequentially linked and the other two of which are lying on two different chains. While the contribution from the diagram k diverges in the thermodynamic limit (as shown below), the cumulant diagram $k^{(c)}$ is an extensive quantity. The definition of $k^{(c)}$ is provided by the sum of contributions [from the expansion of the logarithm in (2.18) in a Taylor series], which have the same set of bonds as the leading diagram k

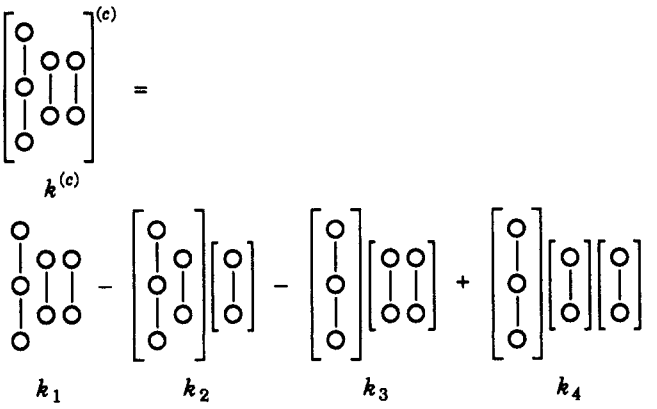

(B.1)

Diagram k_1 is just the diagram k of Figure 2 and diagrams k_2, k_3, and k_4 are constructed from diagrams a, b, and d in Figure 2 and the one-bond diagram[8] (which is of order N_l^0 and therefore does not contribute separately to the packing entropy). Equation B.1 simplifies considerably by excluding from $d_B^{(k_j)}$ [see (2.16)] all contracted diagrams containing the one-bond contraction $R_{1,1}$ (i.e., diagrams $R_{4,4}$ and $R_{4,5}$ of ref 8) as these contributions cancel identically in (B.1). This also means that contributions from the diagrams k_2 and k_4 vanish in the thermodynamic limit. Thus, the cumulant diagram $k^{(c)}$ is reduced to evaluating only diagrams k_1 and k_3

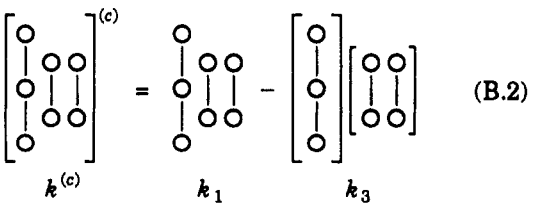

(B.2)

The lattice dependent quantities $d_B^{(k_1)}$ and $d_B^{(k_3)}$ can be determined by using the $R_{B,c}$ from ref 8. Since the contracted diagrams $R_{4,4}$ and $R_{4,5}$ are proportional to $R_{1,1}$, we discard them and thereby obtain

$$d_B^{(k_1)} = -2R_{4,1} - 8R_{4,2} + 48R_{4,3} + \dots = -2N_l^6/z^2 + 24N_l^5/z^2 + \dots \quad (B.3a)$$

$$d_B^{(k_3)} = -2R_{4,1} + \dots = -2N_l^6/z^2 + \dots \quad (B.3b)$$

where ... denotes lower order terms in N_l as well as terms of order z^0, z^{-1}, and z^{-3}, which either cancel in (B.2) (z^0,z^{-1}) or are neglected (z^{-3}) here.

For a mixture, each disconnected part of a diagram may belong to any component, producing many diagrams with the same bond topology but differing only in the labeling of the polymer species. To generalize diagrams k_1 and k_3 to the multicomponent case, we introduce a sequential counting index λ to label diagrams within a given topological group. Thus, we have diagrams $k_{1,\lambda}$ and $k_{3,\lambda}$. Those arising for a binary polymer blend are as follows: The first case has all chains of species 1

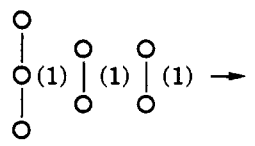

$k_{1,1}$

$$\frac{\left[N_1^{(1)}\right]^2 n_1(n_1-1)N_2^{(1)}(n_1-2)}{2!N_l(N_l-1)(N_l-2)(N_l-3)(N_l-4)(N_l-5)(N_l-6)} \times$$

$$[-2N_l^6/z^2 + 24N_l^5/z^2] \rightarrow \frac{\left[N_1^{(1)}\right]^2 N_2^{(1)}(n_1^3 - 3n_1^2)}{N_l^7(1-21/N_l+\cdots)} \times$$

$$[-N_l^6/z^2 + 12N_l^5/z^2] \rightarrow \frac{\left[N_1^{(1)}\right]^2 N_2^{(1)}(\phi_1^3 - 3M_1\phi_1^2)}{M_1^3} \times$$

$$[-(1+21/N_l)N_l^2/z^2 + 12N_l/z^2] \rightarrow$$

$$N(1,1)^2N(2,1)[-N_l^2\phi_1^3/z^2 - 9N_l\phi_1^3/z^2 + 3N_lM_1\phi_1^2/z^2] \quad \text{(B.4a)}$$

where the notation $N(i,\mu) \equiv N_i^{(\mu)}/M_\mu$ is employed in (B.4–B.6). The case where all chains are species 2 follows as

$$k_{1,2}\text{(i.e., } k_{1,1} \text{ with } 1 \leftrightarrow 2) \rightarrow N(1,2)^2N(2,2)[-N_l^2\phi_2^3/z^2 - 9N_l\phi_2^3/z^2 + 3N_lM_2\phi_2^2/z^2] \quad \text{(B.4b)}$$

The arrows in (B.4) and (B.5) below indicate that only terms surviving in the thermodynamic limit are retained. Mixed-species diagrams are evaluated as

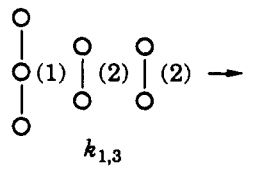

$k_{1,3}$

$$\frac{\left[N_1^{(2)}\right]^2 n_2(n_2-1)N_2^{(1)}n_1}{2!N_l(N_l-1)(N_l-2)(N_l-3)(N_l-4)(N_l-5)(N_l-6)} \times$$

$$[-2N_l^6/z^2 + 24N_l^5/z^2] \rightarrow$$

$$N(1,2)^2N(2,1)[-N_l^2\phi_1\phi_2^2/z^2 - 9N_l\phi_1\phi_2^2/z^2 + N_lM_2\phi_1\phi_2/z^2] \quad \text{(B.4c)}$$

$$k_{1,4}\text{(i.e., } k_{1,3} \text{ with } 1 \leftrightarrow 2) \rightarrow N(1,1)^2N(2,2)[-N_l^2\phi_1^2\phi_2/z^2 - 9N_l\phi_1^2\phi_2/z^2 + N_lM_1\phi_1\phi_2/z^2] \quad \text{(B.4d)}$$

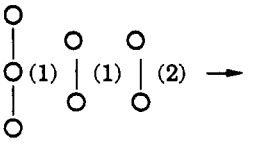

$k_{1,5}$

$$\frac{N_1^{(1)}n_1N_1^{(2)}n_2N_2^{(1)}(n_1-1)}{N_l(N_l-1)(N_l-2)(N_l-3)(N_l-4)(N_l-5)(N_l-6)} \times$$

$$[-2N_l^6/z^2 + 24N_l^5/z^2] \rightarrow$$

$$N(1,1)N(1,2)N(2,1)[-2N_l^2\phi_1^2\phi_2/z^2 - 18N_l\phi_1^2\phi_2/z^2 + 2N_lM_1\phi_1\phi_2/z^2] \quad \text{(B.4e)}$$

$$k_{1,6}\text{(i.e., } k_{1,5} \text{ with } 1 \leftrightarrow 2) \rightarrow N(1,1)N(1,2)N(2,2) \times [-2N_l^2\phi_1\phi_2^2/z^2 - 18N_l\phi_1\phi_2^2/z^2 + 2N_lM_2\phi_1\phi_2/z^2] \quad \text{(B.4f)}$$

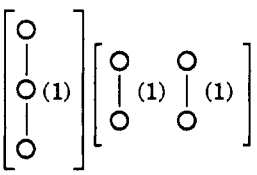

$k_{3,1}$

$$\frac{\left[N_1^{(1)}\right]^2 n_1(n_1-1)N_2^{(1)}n_1}{2!N_l(N_l-1)(N_l-2)N_l(N_l-1)(N_l-2)(N_l-3)} \times$$

$$[-2N_l^6/z^2] \rightarrow \frac{\left[N_1^{(1)}\right]^2 N_2^{(1)}[n_1^3 - n_1^2]}{N_l^7(1-9/N_l+\cdots)} [-2N_l^6/z^2] \rightarrow$$

$$\frac{\left[N_1^{(1)}\right]^2 N_2^{(1)}(\phi_1^3 - \phi_1^2M_1)}{M_1^3} [(1+9/N_l)(-N_l^2/z^2)] \rightarrow$$

$$N(1,1)^2N(2,1)[-N_l^2\phi_1^3/z^2 - 9N_l\phi_1^3/z^2 + N_lM_1\phi_1^2/z^2] \quad \text{(B.5a)}$$

$$k_{3,2}\text{(i.e., } k_{3,1} \text{ with } 1 \leftrightarrow 2) \rightarrow N(1,2)^2N(2,2)[-N_l^2\phi_2^3/z^2 - 9N_l\phi_2^3/z^2 + N_lM_2\phi_2^2/z^2] \quad \text{(B.5b)}$$

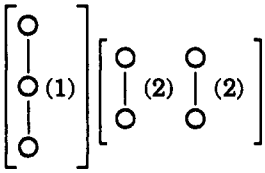

$k_{3,3}$

$$\frac{\left[N_1^{(2)}\right]^2 n_2(n_2-1)N_2^{(1)}n_1}{2!N_l(N_l-1)(N_l-2)N_l(N_l-1)(N_l-2)(N_l-3)} [-2N_l^6/z^2] \rightarrow$$

$$N(2,1)N(1,2)^2[-N_l^2\phi_1\phi_2^2/z^2 - 9N_l\phi_1\phi_2^2/z^2 + N_lM_2\phi_1\phi_2/z^2] \quad \text{(B.5c)}$$

$$k_{3,4}\text{(i.e., } k_{3,3} \text{ with } 1 \leftrightarrow 2) \rightarrow N(1,1)^2N(2,2)[-N_l^2\phi_1^2\phi_2/z^2 - 9N_l\phi_1^2\phi_2/z^2 + N_lM_1\phi_1\phi_2/z^2] \quad \text{(B.5d)}$$

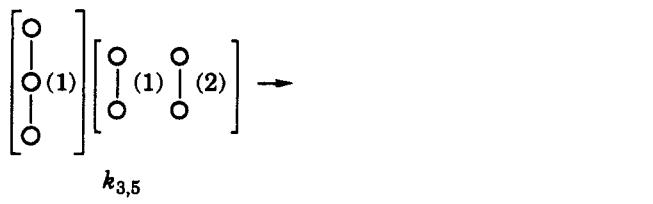

$$\frac{N_1^{(1)}n_1N_1^{(2)}n_2N_2^{(1)}n_1}{N_l(N_l-1)(N_l-2)N_l(N_l-1)(N_l-2)(N_l-3)}\,[-2N_l^6/z^2] \rightarrow$$

$$N(1,1)N(1,2)N(2,1)[-2N_l^2\phi_1^2\phi_2/z^2 - 18N_l\phi_1^2\phi_2/z^2] \quad \text{(B.5e)}$$

$$k_{3,6}(\text{i.e, } k_{3,5} \text{ with } 1 \leftrightarrow 2) \rightarrow N(1,1)N(1,2)N(2,2) \times [-2N_l^2\phi_1\phi_2^2/z^2 - 18N_l\phi_1\phi_2^2/z^2] \quad \text{(B.5f)}$$

Although all diagrams in (B.4) and (B.5) contain hyperextensive contributions of order N_l^2, the cumulant diagram $k^{(c)}$ in the thermodynamic limit yields as the leading term only the extensive contribution, proportional to N_l, of

$$k^{(c)} = \sum_{\lambda=1}^{6}(k_{1,\lambda} - k_{3,\lambda}) \rightarrow 2\frac{N_l}{z^2}[N(1,1)\phi_1 + N(1,2)\phi_2] \times [N(1,1)N(2,1)M_1\phi_1 + N(1,2)N(2,2)M_2\phi_2] \quad \text{(B.6)}$$

However, the result (B.6) diverges in the long-chain limit ($M_1, M_2 \rightarrow \infty$). Contributions from both diagrams k and l of Figure 2 must be added together to produce a finite value in this long-chain limit. Diagrams k and l have rather similar topologies. The latter contains contributions from distant bonds on a single chain that must be combined with similar groups of bonds on different chains to yield physically meaningful results. The same cancellation of singularities in the $M_1, M_2 \rightarrow \infty$ limit occurs in all diagrams containing the nonsequential counting indexes $N_{i,j}^{(\mu)}$ and comes from the physical indistinguishability between distant units on the same chain and those on different chains for melts, blends, etc.[1]

Appendix C: Multicomponent System Energy Diagrams

Details of the evaluation[26] of energy diagrams containing only interaction lines are provided by Appendix A of ref 10. Here we illustrate the counting process for those energy diagrams that also contain correlating bonds. The computations described below are illustrated for a binary system and the particular diagram d_{10} (see Figure 4) with two correlating bonds lying on different chains and two interaction lines. Generalization to a multicomponent system follows directly. In order to avoid confusion between the symbols d_{10} and d_B, the diagram d_{10} is here designated as t. The expansion of the logarithm of (3.6) in a Taylor series determines the cumulant diagram $t^{(c)}$ as

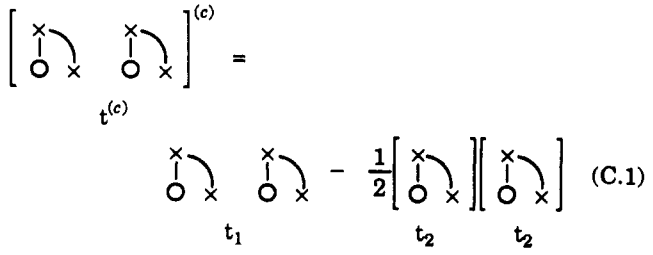

(C.1)

The factors d_B for the diagrams t_1 and t_2 may be obtained from Table II of ref 8 because an interaction line contributes to d_B indentically as a correlating bond

$$d_B^{(t_1)} = R_{4,1} + 2R_{4,2} - 13R_{4,3} + \ldots = [N_l^6/z^2 - 7N_l^5/z^2] + \ldots \quad \text{(C.2)}$$

$$d_B^{(t_2)} = R_{2,1} + \ldots = [N_l^3/z] + \ldots \quad \text{(C.3)}$$

where ... denotes lower order terms in N_l and terms of order z^0, z^{-1}, and z^{-3}, which either cancel in (C.1) or are neglected (z^{-3}). Bonds and uncorrelated monomers of diagrams t_1 and t_2 may correspond to either polymer species in the system. A binary blend produces 10 different diagrams $t_{1,j}$, $t_{2,j}$ (and $t_j^{(c)}$), which are labeled here by a sequential counting index j. Their contributions are evaluated as

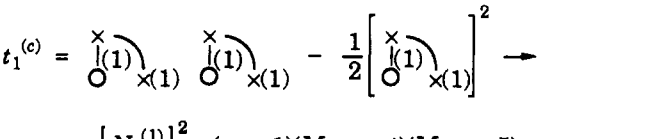

$$\frac{[N_1^{(1)}]^2n_1(n_1-1)(M_1n_1-4)(M_1n_1-5)}{2!2!N_l(N_l-1)(N_l-2)(N_l-3)(N_l-4)(N_l-5)} \times \left[\frac{\varepsilon_{11}z}{N_l}\right]^2 \{8\}[N_l^6/z^2 - 7N_l^5/z^2] -$$

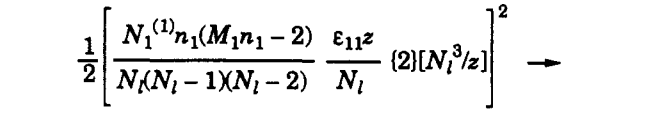

$$N(1,1)^2N_l\varepsilon_{11}^2[4\phi_1^4 - 10\phi_1^3 - 2M_1\phi_1^3] \quad \text{(C.4a)}$$

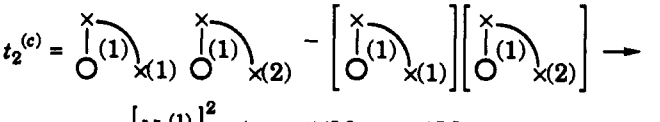

$$\frac{[N_1^{(1)}]^2n_1(n_1-1)(M_1n_1-4)M_2n_2}{2!N_l(N_l-1)(N_l-2)(N_l-3)(N_l-4)(N_l-5)} \times \frac{\varepsilon_{11}\varepsilon_{12}z^2}{N_l^2}\{8\}[N_l^6/z^2 - 7N_l^5/z^2] - \frac{N_1^{(1)}n_1(M_1n_1-2)}{N_l(N_l-1)(N_l-2)} \times \frac{\varepsilon_{11}z}{N_l}\{2\}[N_l^3/z]\frac{N_1^{(1)}n_1M_2n_2}{N_l(N_l-1)(N_l-2)}\frac{\varepsilon_{12}z}{N_l}\{2\}[N_l^3/z] \rightarrow$$

$$N(1,1)^2N_l\varepsilon_{11}\varepsilon_{12}[8\phi_1^3\phi_2 - 8\phi_1^2\phi_2 - 4M_1\phi_1^2\phi_2] \quad \text{(C.4b)}$$

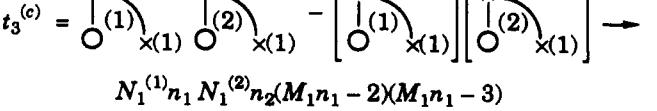

$$\frac{N_1^{(1)}n_1N_1^{(2)}n_2(M_1n_1-2)(M_1n_1-3)}{2!N_l(N_l-1)(N_l-2)(N_l-3)(N_l-4)(N_l-5)} \times \frac{\varepsilon_{11}\varepsilon_{12}z^2}{N_l^2}\{8\}[N_l^6/z^2 - 7N_l^5/z^2] - \frac{N_1^{(1)}n_1(M_1n_1-2)}{N_l(N_l-1)(N_l-2)} \times \frac{\varepsilon_{11}z}{N_l}\{2\}[N_l^3/z]\frac{N_1^{(2)}n_2M_1n_1}{N_l(N_l-1)(N_l-2)}\frac{\varepsilon_{12}z}{N_l}\{2\}[N_l^3/z] \rightarrow$$

$$N(1,1)N(1,2)N_l\varepsilon_{11}\varepsilon_{12}[8\phi_1^3\phi_2 - 12\phi_1^2\phi_2] \quad \text{(C.4c)}$$

$t_4^{(c)}$ = 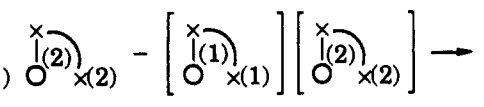 →

$$\frac{N_1^{(1)}n_1\,N_1^{(2)}n_2(M_1n_1-2)(M_2n_2-2)}{N_l(N_l-1)(N_l-2)(N_l-3)(N_l-4)(N_l-5)}\;\frac{\epsilon_{11}\epsilon_{22}z^2}{N_l^2}\times$$

$$\{4\}[N_l^6/z^2-7N_l^5/z^2]\;-\;\frac{N_1^{(1)}n_1(M_1n_1-2)}{N_l(N_l-1)(N_l-2)}\;\frac{\epsilon_{11}z}{N_l}\times$$

$$\{2\}[N_l^3/z]\;\frac{N_1^{(2)}n_2(M_2n_2-2)}{N_l(N_l-1)(N_l-2)}\;\frac{\epsilon_{22}z}{N_l}\;\{2\}[N_l^3/z]\longrightarrow$$

$$8N(1,1)N(1,2)N_l\epsilon_{11}\epsilon_{22}\phi_1{}^2\phi_2{}^2 \quad \text{(C.4d)}$$

$t_5^{(c)}$ = 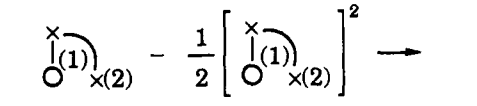 →

$$\frac{\left[N_1^{(1)}\right]^2 n_1(n_1-1)M_2n_2(M_2n_2-1)}{2!2!N_l(N_l-1)(N_l-2)(N_l-3)(N_l-4)(N_l-5)}\times$$

$$\left[\frac{\epsilon_{12}z}{N_l}\right]^2\{8\}[N_l^6/z^2-7N_l^5/z^2]\;-$$

$$\frac{1}{2}\left[\frac{N_1^{(1)}n_1M_2n_2}{N_l(N_l-1)(N_l-2)}\;\frac{\epsilon_{12}z}{N_l}\;\{2\}[N_l^3/z]\right]^2\longrightarrow$$

$$N(1,1)^2N_l\epsilon_{12}^2[4\phi_1{}^2\phi_2{}^2-2\phi_1{}^2\phi_2-2M_1\phi_1\phi_2{}^2] \quad \text{(C.4e)}$$

$t_6^{(c)}$ = 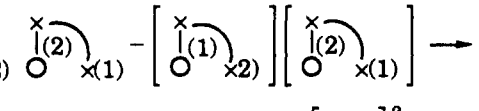 →

$$\frac{N_1^{(1)}n_1\,N_1^{(2)}n_2(M_2n_2-2)(M_1n_1-2)}{N_l(N_l-1)(N_l-2)(N_l-3)(N_l-4)(N_l-5)}\left[\frac{\epsilon_{12}z}{N_l}\right]^2\times$$

$$\{4\}[N_l^6/z^2-7N_l^5/z^2]\;-\;\frac{N_1^{(1)}n_2M_1n_1}{N_l(N_l-1)(N_l-2)}\;\frac{\epsilon_{12}z}{N_l}\times$$

$$\{2\}[N_l^3/z]\frac{N_1^{(2)}n_2M_1n_1}{N_l(N_l-1)(N_l-2)}\;\frac{\epsilon_{12}z}{N_l}\;\{2\}[N_l^3/z]\longrightarrow$$

$$N(1,1)N(1,2)N_l\epsilon_{12}^2[\,8\phi_1{}^2\phi_2{}^2-8\phi_1\phi_2{}^2-8\phi_1{}^2\phi_2] \quad \text{(C.4f)}$$

$t_7^{(c)}$ (i.e., $t_3^{(c)}$ with $1 \leftrightarrow 2$) $\rightarrow N(1,1)N(1,2)N_l\epsilon_{12}\epsilon_{22}[8\phi_1\phi_2^3-12\phi_1\phi_2^2]$ (C.4g)

$t_8^{(c)}$ (i.e., $t_5^{(c)}$ with $1 \leftrightarrow 2$) $\rightarrow N(1,2)^2N_l\epsilon_{12}^2[4\phi_1^2\phi_2^2-2\phi_1\phi_2^2-2M_2\phi_1^2\phi_2]$ (C.4h)

$t_9^{(c)}$ (i.e., $t_2^{(c)}$ with $1 \leftrightarrow 2$) $\rightarrow N(1,2)^2N_l\epsilon_{12}\epsilon_{22}[8\phi_1\phi_2^3-8\phi_1\phi_2^2-4M_2\phi_1\phi_2^2]$ (C.4i)

$t_{10}^{(c)}$ (i.e., $t_1^{(c)}$ with $1 \leftrightarrow 2$) $\rightarrow N(1,2)^2N_l\epsilon_{22}^2[4\phi_2^4-10\phi_2^3-2M_2\phi_2^3]$ (C.4j)

where $N(i,\mu) \equiv N_i^{(\mu)}/M_\mu$. The symmetry numbers s_D for the diagrams $t_{1,j}$ and $t_{2,j}$ are introduced in eqs C.4a–C.4j in braces to help an interested reader follow this aspect of the calculations. The value of the cumulant diagram $t^{(c)}$ is the sum of contributions C.4a–C.4j

$$t^{(c)} = \sum_{j=1}^{10} t_j^{(c)} \quad \text{(C.5)}$$

The long-chain limit, M_1, $M_2 \rightarrow \infty$, of diagrams $t_1^{(c)}$, $t_2^{(c)}$, $t_5^{(c)}$, $t_8^{(c)}$, $t_9^{(c)}$, and $t_{10}^{(c)}$ produces unbounded result, but the offending divergences are removed when their contributions are added to those of diagrams e_5 of Figure 4.

References and Notes

(1) Flory, P. J. *Principles of Polymer Chemistry*; Cornell University Press: Ithaca, NY, 1953.

(2) Han, C. C.; Baurer, B. J.; Clark, J. C.; Muroga, Y.; Matsushita, Y.; Okada, M.; Tran-Cong, Q.; Sanchez, I. C. *Polymer* **1988**, *29*, 2002.

(3) Bates, F. S.; Muthukumar, M.; Wignall, G. D.; Fetters, L. J. *J. Chem. Phys.* **1988**, *89*, 535. Bates, F. S.; Fetters, L. J.; Wignall, G. D. *Macromolecules* **1988**, *21*, 1086. Ito, H.; Russel, T. P.; Wignall, G. D. *Macromolecules* **1987**, *20*, 2213. Murray, C. T.; Gilmer, J. W.; Stein, R. S. *Macromolecules* **1985**, *18*, 996.

(4) Freed, K. F. *J. Phys. A* **1985**, *18*, 871.

(5) Bawendi, M. G.; Freed, K. F.; Mohanty, U. *J. Chem. Phys.* **1986**, *84*, 7036; **1987**, *87*, 5534.

(6) Bawendi, M. G.; Freed, K. F. *J. Chem. Phys.* **1988**, *88*, 2741.

(7) Pesci, A. I.; Freed, K. F. *J. Chem. Phys.* **1989**, *90*, 2003.

(8) Nemirovsky, A. M.; Bawendi, M. G.; Freed, K. F. *J. Chem. Phys.* **1987**, *87*, 7272.

(9) Mayer, J. E.; Mayer, M. G. *Statistical Mechanics*; Wiley: New York, 1940.

(10) Dudowicz, J.; Freed, K. F.; Madden, W. G. *Macromolecules* **1990**, *23*, 4803.

(11) *Polymer Handbook*; Brandup, J., Immergut, E. H., Eds., Wiley: New York, 1975.

(12) Freed, K. F. *J. Chem. Phys.* **1988**, *88*, 5871.

(13) Guggenheim, E. A. *Mixtures*; Oxford University Press: Oxford, U.K., 1952. Prigogine, I. *The Molecular Theory of Solutions*; North-Holland: Amsterdam, 1957.

(14) The term *excess* free volume is introduced to emphasize that this free volume ϕ_v may be removed by an increase of pressure until a close-packed state is reached with $\phi_v \rightarrow 0$. Consequently, the physical interpretation of the excess free volume is represented by the expression $\phi_v V = V - V^*$ with V^* the analog of the closed-packing volume in continuum model theories.

(15) Freed, K. F.; Pesci, A. I. *Macromolecules* **1989**, *22*, 4048.

(16) Shiomi, T.; Hamada, F.; Nasako, T.; Yoneda, K.; Imai, K.; Nakajima, A. *Macromolecules* **1990**, *23*, 229.

(17) Kubo, R. *J. Phys. Soc. Jpn.* **1962**, *17*, 1100.

(18) Diagrams *o* and *q* in Figure 6 of ref 8 are identical, and there is only one corresponding combinatorial factor $N_\perp^{(\mu)}$ replacing the sum of $N_\perp^{(\mu)}$ and $N_{\perp\prime}^{(\mu)}$ in ref 8. The corrected values of $N_{\perp\prime}^{(\mu)}$ for architectures *a–c* are $N_{\perp\prime}^{(\mu)} = 0$, $N_{\perp\prime}^{(\mu)} = 4(N_\mu - 2)$, and $N_{\perp\prime}^{(\mu)} = 18(N_\mu - 2)$, respectively.

(19) Flory, P. J. *Discuss. Faraday Soc.* **1970**, *49*, 7.

(20) Rowlinson, J. S. *Liquids and Liquid Mixtures*; Butterworths: London, 1969.

(21) Schweizer, K. S.; Curro, J. G. *J. Chem. Phys.* **1989**, *91*, 5059.

(22) Bawendi, M. G.; Freed, K. F. *J. Chem. Phys.* **1987**, *86*, 3720.

(23) Dickman, R.; Hall, C. K. *J. Chem. Phys.* **1986**, *85*, 4108.

(24) Honnell, K. G.; Hall, C. K. *J. Chem. Phys.* **1989**, *90*, 1841.

(25) Dee, G. T.; Walsh, D. J. *Macromolecules* **1988**, *21*, 815.

(26) The symmetry number s_D for diagrams having only interaction lines (see Table V of ref 10) is defined as the product of factors $1/2$ for each separate, disconnected part of a given diagram and a factor of $1/n!$ representing the indistinguishability of any n identical portions of the diagram.